Geologica Acta, Vol.12, Nº 2, June 2014, 151-170
DOI: 10.1344/105.000002081

geologica acta

Petrogenesis of Miocene volcanic arc rocks over the Chilean-Pampean flat-slab segment of the Central Andes constrained by mineral chemistry

V.D. LITVAK[1] and **S. POMA**[2]

[1]**Instituto de Estudios Andinos Don Pablo Groeber, Departamento de Geología**
Facultad de Ciencias Exactas y Naturales, Universidad de Buenos Aires-CONICET Ciudad Universitaria, Pabellón II, 1428, Ciudad de Buenos Aires, Argentina. E-mail: vane@gl.fcen.uba.ar. Phone: +54-11-4576-3329

[2]**Instituto de Geociencias Básicas, Aplicadas y Ambientales de Buenos Aires**
Departamento de Geología, Facultad de Ciencias Exactas y Naturales, Universidad de Buenos Aires-CONICET. Ciudad Universitaria, Pabellón II, 1428, Ciudad de Buenos Aires, Argentina. E-mail: stella@gl.fcen.uba.ar

ABSTRACT

Miocene arc volcanism is manifested widely in the Valle del Cura-El Indio belt region (29°30´–30° South latitude), in the southern Central Andes of Argentina and Chile. The magmas that fed this volcanism are well represented by the Cerro de las Tórtolas Formation, which is divided into two volcanic episodes based on petrographic, chemical and age differences: an older basaltic-andesitic event (16–14Ma) and a younger andesitic to dacitic (13–10Ma) one. Representative plagioclase, orthopyroxene, clinopyroxene and amphibole phenocrysts from rock samples already characterized from geochemical and isotopic viewpoints were selected for electron microprobe determination of mineral chemistry. Results indicate an overall homogeneous composition for each of the mineral phases. Equilibrium temperatures were estimated through two-pyroxenes, amphibole-plagioclase and amphibole geothermometers, which show a consistent temperature range between 970 to 850°C. Equilibrium pressure calculated using amphibole composition for volcanic suites produced the most comprehensive results for pressure equilibrium conditions, with results close to 4kb. Changes in the residual mineral assemblages and variations in isotopic signatures indicate that primary magmas were equilibrated at the lower crust with a gradual increase of crustal thickness. These melts evolved towards intermediate magma chambers, where crystallization of phenocrysts occurred at the same temperature and pressure conditions, hence, no increase in depth of intermediate magma chambers is registered although the increase of crustal thickness registered from Lower to Middle Miocene times.

KEYWORDS **Andesitic. Geothermobarometry. Volcanism. Crustal thickness. Valle del Cura. Argentina. Chile.**

INTRODUCTION

Geochemical features of arc-related volcanic rocks provide information about tectonic conditions beneath active volcanic arcs. These tectonic processes have a strong influence on the genesis, evolution and final products of the resulting volcanic rocks. During the late Oligocene (25Ma) the tectonic configuration of the southern Central Andean margin was marked by the break up of the Farellón plate into the Nazca and Cocos plates, which resulted in changes to the orthogonal convergence direction at increased subduction rates (*e.g.* Pardo-Casas and Molnar, 1987; Barckhausen *et al.*, 2008). Under these conditions an Andean type arc was developed and concomitant magmatic activity was almost continuous until the Upper Miocene when volcanism ended due to the shallowing of the downgoing slab at the present-day Pampean flat slab segment (Fig. 1) (Kay *et* *al*., 1987; Ramos *et al*., 1989, 2002; Kay and Mpodozis, 2002). A peak of this arc volcanism is well represented in the Valle del Cura region over the Pampean flat slab-segment producing andesitic to dacitic lava flows of Lower to Middle Miocene age, being part of the Cerro de las Tórtolas Formation (Kay *et al*., 1987, 1991; Maksaev *et al*., 1984). The chemical evolution of all this Tertiary magmatism and its tectonic framework was mainly controlled by changes in the geometry of the downgoing slab (Kay *et al*., 1987, 1991, 1999; Bissig *et al*., 2003; Litvak *et al*., 2007, Litvak and Poma 2010).

The main focus of this work is to gain insight into the Lower to Middle Miocene andesitic to dacitic volcanic rocks of the Cerro de las Tórtolas Formation. We aim to understand the genesis of their melts and the evolution towards their final products by means of an integrated and detailed study on the petrogenesis of Miocene volcanic arc rocks from the Valle del Cura region, particularly with mineral chemistry data. A P-T analysis of the new electron microprobe data for the investigated samples, together with their petrographic and geochemical characteristics, allows the identification of differences within this Miocene magmatism and the evaluation of whether major regional tectonic configuration or localized factors have influenced its evolution and the finally resulting rocks.

GEOLOGICAL AND GEOCHRONOLOGICAL OUTLINES OF MIOCENE ARC VOLCANISM

The andesitic volcanism products of Cerro las Tórtolas Formation crop out along the Valle del Cura region, which is located over the presently volcanically inactive Pampean flat slab segment of the southern Central Andes (Fig. 1). The Valle del Cura constitutes a mineralized hydrothermal system that, together with the El Indio belt in Chile, forms a north-south-trending block limited by high-angle reverse faults (Jones *et al*., 1996; Martin *et al*., 1997a). This area is characterized by a thick sequence of Tertiary volcanic and volcaniclastic arc-like rocks that are associated with both Au-Ag-Cu-rich epithermal and porphyry-type mineral deposits (Maksaev *et al*., 1984; Kay *et al*., 1987, 1991; Ramos *et al*., 1989; Nasi *et al*., 1990; Bissig *et al*., 2001; Litvak and Page, 2002; Litvak and Poma, 2005; Litvak *et al*., 2004; Litvak, 2009). The studied area corresponds to the Argentine slope of the El Indio-Valle del Cura belt (Fig. 2). The stratigraphic column in the area includes a Permo-Triassic sedimentary, plutonic, and volcanic basement unconformably overlain by Tertiary sedimentary and volcanic rocks. Paleocene to Lower Miocene volcanic rocks belong to three main volcanic events: i) a volumetrically small Paleocene alkaline mafic magmatic event radiometrically dated at 55.9 ± 1.9Ma (Litvak and Page, 2002); ii) a thick Eocene to Lower Oligocene event characterized by a backarc volcanic and sedimentary sequence that includes tuffs, conglomerates, volcanic arenites, and volcanic and volcaniclastic products such as dacitic ignimbrites and rhyolite lava flows, with a K/Ar age range from 44 to 36Ma (Limarino *et al*., 1999; Litvak and Poma 2005); and iii) a Lower Oligocene-Early Miocene areally widespread and large-volume arc-type magmatic event that generated products of bimodal composition, including a first volcanic event composed

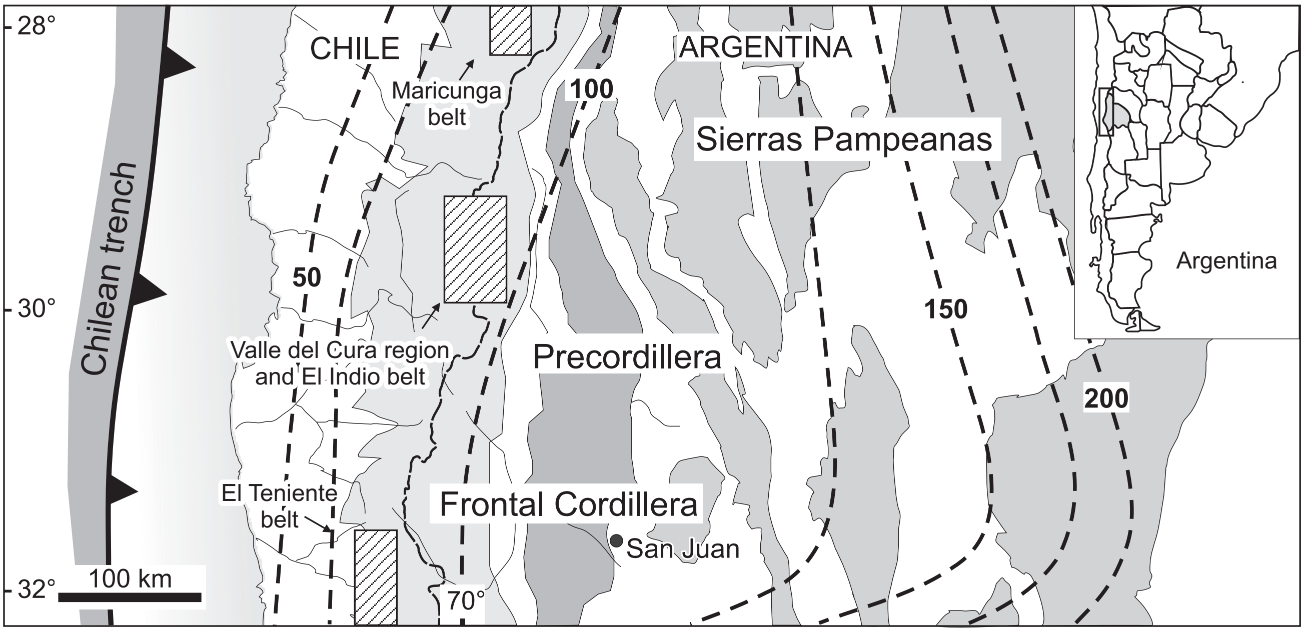

FIGURE 1. Valle del Cura and the El Indio belt locations at the Pampean (Chilean) flat slab segment, Southern Central Andes. Dashed lines show subducted slab depth.

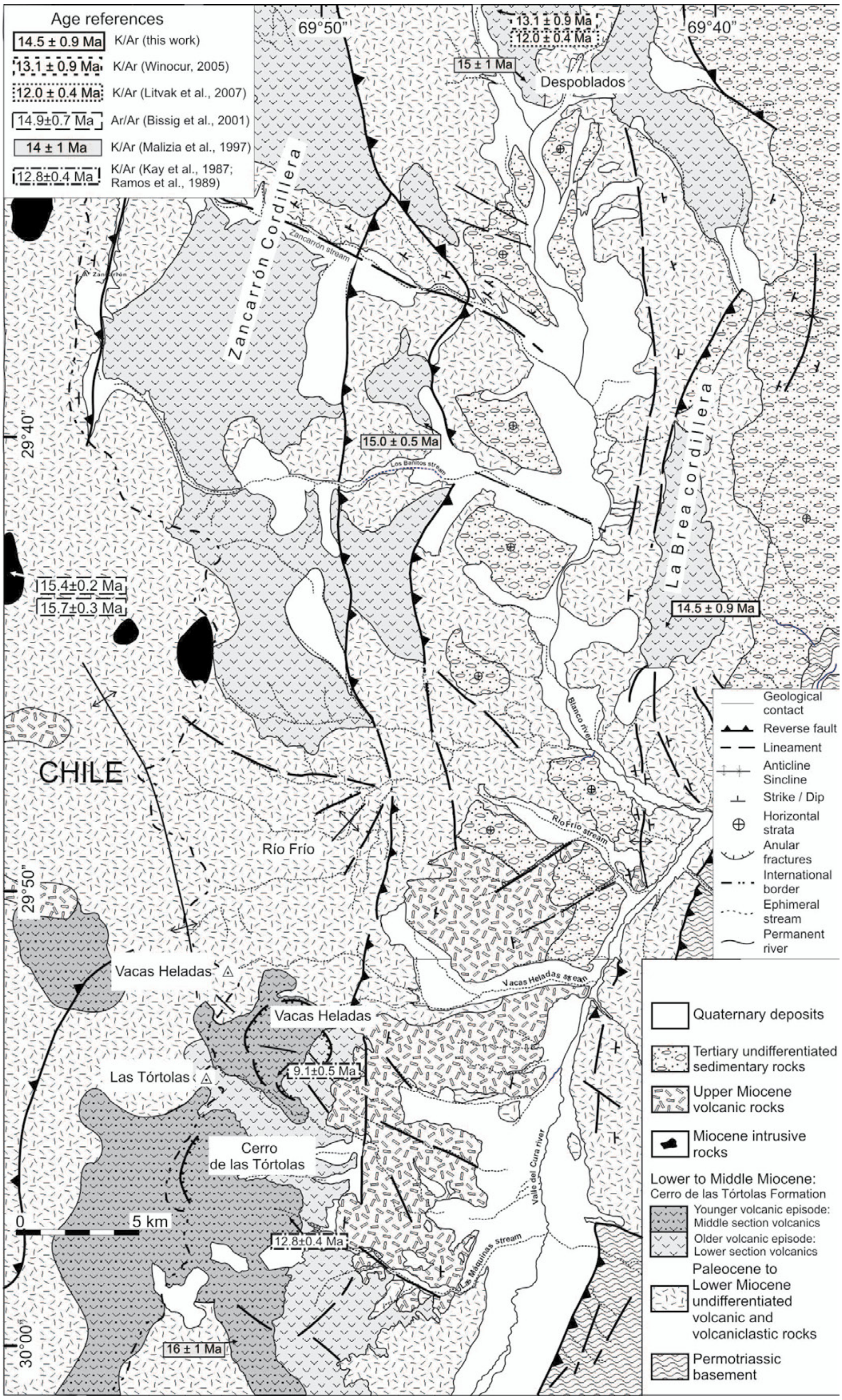

FIGURE 2. Simplified geological map of the central and southern area of the Valle del Cura region-El Indio belt (geology for Argentina side is modified after Litvak *et al.*, 2007, Litvak and Poma, 2010; that for Chile side is from Nasi *et al.*, 1990 and Martin *et al.*, 1997).

of dacites to rhyolites lavas and ignimbrites, and a second one, composed of basaltic to andesitic lava flows. Reported ages for both events include a range of 25.1 to 17.6Ma (Maksaev *et al*., 1984; Nasi *et al*., 1990; Martin *et al*., 1997b; Bissig *et al*., 2001; Litvak *et al*., 2005b; Litvak, 2009). Recently reported $^{40}Ar/^{39}Ar$ dating on presumed Eocene volcaniclastic rocks yielded ages between 18 and 24Ma, indicating that this volcanic activity is younger and related to the Late Oligocene-Early Miocene arc-type magmatic event (Winocur *et al*., 2014). Younger magmatism, of Upper Miocene age, represented by explosive rhyolitic products and minor rhyolitic arc-type lavas mark the end of volcanic activity in the area (Ramos *et al*., 1989; Kay *et al*., 1991; Bissig *et al*., 2001, 2003). Tertiary sedimentary sequences and Quaternary deposits complete the stratigraphy of the area (Fig. 2).

The Lower to Middle Miocene volcanism of Cerro the las Tórtolas Formation, which constitutes the focus of this work, represents the volcanic arc activity that took place along the border and in the Valle del Cura area. The main outcrops occur in the Cerro de las Tórtolas and Vacas Heladas volcanoes that are the main volcanic centers related to this volcanism in the southern Valle del Cura area. Ramos *et al*. (1989) recognized two sequences of lavas for these stratovolcanos and divided the volcanic unit on the basis of petrographic, chemical and age characteristics into an andesitic to basaltic andesitic lower sequence and a dacitic upper sequence. These two sequences were later recognized along the Valle del Cura region and on the Chilean side of the Andes cordillera where a compilation of K/Ar, U/Pb and $^{40}Ar/^{39}Ar$ ages indicates ages of 16–14 Ma for the lower sequence and 13–10Ma for the upper sequence (Maksaev *et al*., 1984; Ramos *et al*., 1989; Kay *et al*., 1991, 1999; Martin *et al*., 1997a; Bissig *et al*., 2001; Litvak *et al*., 2005b, 2007; Winocur, 2005).

Thus, two main volcanic episodes are clearly distinguished within the Cerro de las Tórtolas unit, which are represented by the lower and upper sequences of the formation. However, the lithologies included whithin the formation and, particulary the nomenclature used for the younger lavas, have been inconsistent and have changed through time (see Litvak *et al*., 2007 for further discussion on stratigraphy). For that reason, some authors (Kay *et al*., 1999; Bissig *et al*., 2001) have included a series of dacitic crystalline tuffs of 12 to 11Ma as part of the Middle Miocene sequences of Cerro de las Tórtolas Formation, which are formally included in a different stratigraphic unit named Tambo Formation, according to Litvak *et al*. (2004).

The oldest volcanic episode, of Lower Miocene age, is broadly distributed in the southern extreme of the mapped area, at Cerro de las Tórtolas and at Cerro Vacas Heladas, in the Valle del Cura. The two stratovolcanoes formed mainly by andesitic to dacitic lava flows (Fig. 3A). Andesitic lavas of this first volcanic episode are also recognized in the west of the Blanco river (Fig. 2), in the Zancarrón Cordillera and to the east, in the La Brea Cordillera (Fig. 3B, C). There is no clear preserved eruptive center linked to these outcrops in the area. However, Litvak *et al.* (2005a) suggested that Zancarrón Cordillera could be an eroded stratovolcano on the basis of its morphology and particularly from the aeromagnetometry evidence. The andesitic lavas located in La Brea Cordillera form isolated lava flows occurring at the top of the ranges. Considering their low volume, isolated configuration and proximity, they could also be related to the inferred eruptive center of Zancarrón Cordillera. A new whole rock K-Ar age for La Brea Cordillera sequence is presented here. It refers to an andesite from the subhorizontal lava flows that crop out on the top of the cordillera and yielded an age of 14.5 ± 0.9 (Table 1), which confirms a Miocene age of the lavas and its assigment to the older volcanic episode. Northern outcrops belonging to this younger volcanic episode are located in the Despoblados region (Fig. 2), next to La Brea Cordillera, and can also be considered as part of the lava flows derived from the Zancarrón eruptive center. Petrographic features of these products, presented below, will confirm these correlations.

TABLE 1. Whole rock K-Ar age for an andesite from the Cerro de las Tórtolas Formation which crops out at the top of La Brea Cordillera

Sample	Lat/Long	% K	rad. Ar nl/g	% atm. Ar	Age Ma	Error 2 sig.
SP79C	29°43'45"S/ 69°41'53"W	2.375	1.342	74	14.5	0.9

The Late Miocene volcanic episode, represented by the upper sequence of the unit, is volumetrically minor and restricted to the uppermost lava flows of the Vacas Heladas and Cerro de las Tórtolas volcanoes (Figs. 2; 3). Thus, the latter two volcanic centers have the complete volcanic record of both Lower to Middle Miocene andesitic arc volcanism. Miocene lavas crop out at high elevation where they unconformably cover older volcanic and volcaniclastic rocks. They generally present a subhorizontal attitude (Fig. 3B, C) although in some cases they have been tilted by Upper Miocene reverse faults.

PETROGRAPHY

A petrographic description of Miocene arc lava flows is presented in order to show the differences between lavas from the two volcanic episodes represented by the lower and upper sections of Cerro de las Tórtolas Formation. The described samples come from stratovolcanoes and outcrops from the localities mentioned above, as follows: i) the Cerro de las Tórtolas and Vacas Heladas volcanoes,

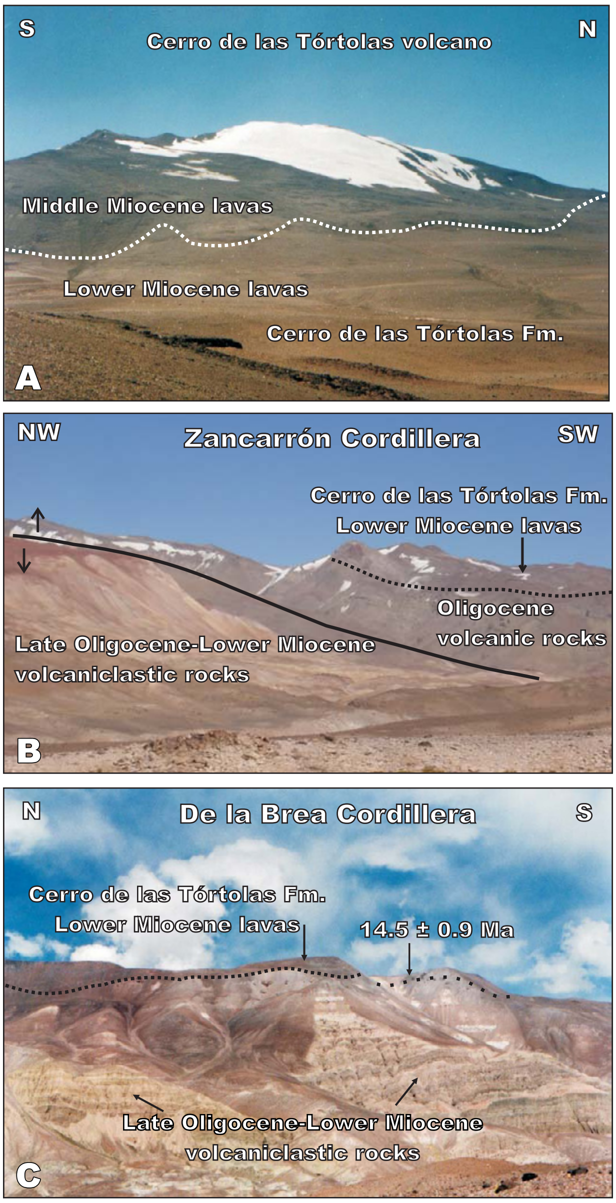

FIGURE 3. Main outcrops of the Cerro de las Tórtolas Formation: A) Cerro de las Tórtolas volcano with high viscosity lavas flows from Middle Miocene units, which covers the uppermost sequences; B) Lower Miocene lavas in Zancarrón Cordillera covers Oligocene volcanic outcrops; C) Thin lava flow from Lower Miocene lavas in La Brea Cordillera, dated in this work.

the Despoblados region and Cordilleras de la Brea and Zancarrón for the lower sequence ii) the uppermost units of the Cerro de las Tórtolas and Vacas Heladas volcanoes for the upper section. Most of the lava flows preserve primary depositional features, such as corded surfaces, vesicular textures and cooling fractures. Rocks from the older volcanic episode are typically light grey porphyritic andesites, with plagioclase phenocrysts. However, younger lavas are dark andesites with higher phenocrysts/groundmass ratios.

Lower Miocene volcanic arc lavas

Andesites from the Cerro de las Tórtolas and Vacas Heladas volcanic centers are porphyritic lavas with 50-60vol% of phenocrysts of plagioclase, orthopyroxene, clinopyroxene and amphibole, in decreasing order of abundance. The groundmass is mostly felty, but hyalopilitic varieties are frequent. Plagioclase is the most abundant mineral; larger crystals have a sieve texture in the glass-rich andesites (Fig. 4A). Composition is andesine (An_{46}, according to the Michel Levy method) although normal and oscillatory zoning is present. Mafic mineral content is approximately 25vol%, the more abundant minerals being orthopyroxene and clinopyroxene. Amphibole is barely present in these andesites. It appears as small prisms (0.3mm) with coarse borders of opaque minerals.

Samples from Zancarrón Cordillera are similar to those previously described. Phenocrysts are present in 30 to 40vol%. (Fig. 4B). The main difference with andesites from the Cerro de las Tórtolas and Vacas Heladas volcanoes is that groundmass is always felty. Andesites from La Brea Cordillera are also porphyritic lavas with almost 50vol% phenocrysts. These are mostly plagioclase, whose larger crystals show in sieve texture. Orthopyroxene and clinopyroxene are the mafic phases present while amphibole is absent in these andesites. The groundmass is felty, but hyalopilitic textures are also shown. An anhedral olivine xenocryst, rounded by small pyroxenes, was found in one of the studied samples of Cordillera del Zancarrón (Fig. 4C).

Other investigated samples are from the Despoblados area. These andesites show petrographical characteristics that are transitional with those of the younger lavas of Cerro de las Tórtolas Formation. They are porphyritic to seriate andesites (30 to 40vol% of phenocrysts) with plagioclase, pyroxene and amphibole phenocrysts (Fig. 4D). In these samples, amphibole is more abundant than pyroxene; in some cases, amphibole is the only mafic mineral present as phenocrysts. Plagioclase is subhedral and larger crystals show sieve textures. Amphiboles appear as euhedral crystals generally rimmed by opaque minerals. Other phenocrysts are made up of orthopyroxene, which is less common and appears as smaller crystals. The groundmass is mostly felty with some hyalopilitic varieties. Accessory minerals are apatite and opaque minerals, which occur as microphenocrysts and in the groundmass.

Middle Miocene volcanic arc lavas

Middle Miocene volcanic arc lavas are typically porphyritic andesites with higher phenocrysts/groundmass ratio (>60vol% of phenocrysts) than the previously described andesites. The main differences are the presence

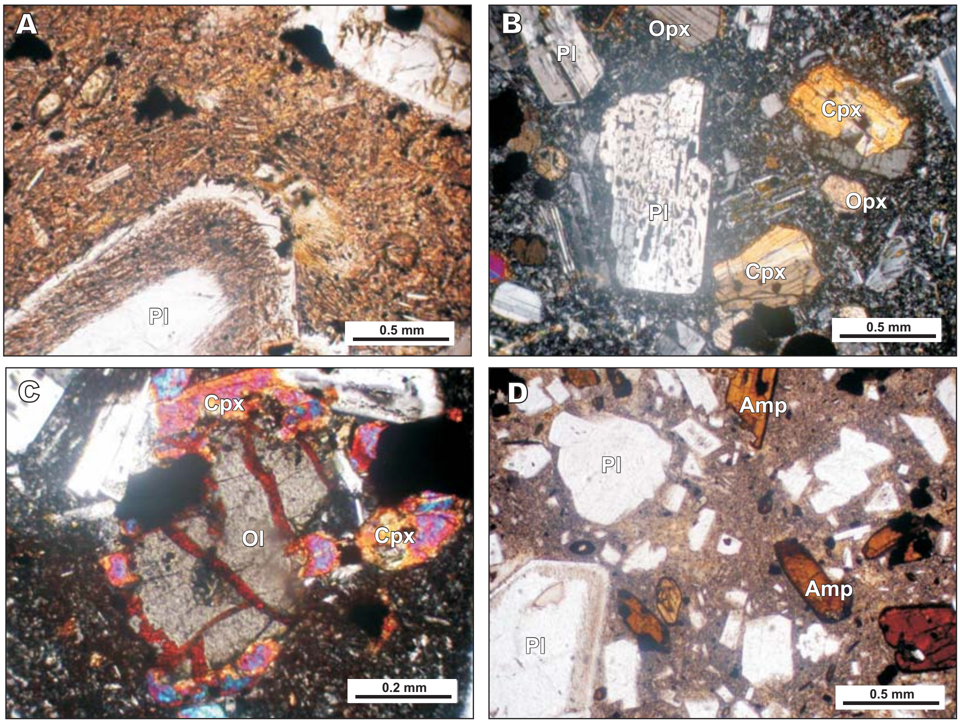

FIGURE 4. Andesites from the Lower Miocene volcanic episode from Cerro de las Tórtolas Formation: A) Plagioclase phenocryst with sieve texture in a hyalopilitic groundmass (Tórtolas volcano); B) Porphyritic varieties with plagioclase, orthopyroxene and clinopyroxene and minor amphibole (Zancarrón Cordillera); cross polarized; C) Olivine xenocryst, rounded by small pyroxenes (Zancarrón Cordillera); cross polarized; D) Porphyritic to seriate andesites with plagioclase, pyroxene and amphibole phenocrysts; the latter more abundant in samples from the Despoblados area, groundmass is hyalopilitic.

of tridimite, amphibole as the most frequent accessory phase and the abundance of volcanic glass. Plagioclase is the most abundant phenocryst. Microphenocrysts form aggregates due to cumulus effects, whereas larger phenocrysts, of andesine composition (An_{48}), have a typical sieve texture with fresh brownish glass inclusions and incipient clay alteration. Amphibole is the most abundant mafic mineral (Fig. 5A) and pyroxene is scarce. In mela-andesites varieties, pyroxene shows a coarse rim of opaque ore and groundmass embayments resulting in skeletal structures (Fig. 5B). An exclusive feature of these andesites is the presence of tridimite in the groundmass (Fig. 5C). The groundmass is usually felty to hyalopilitic; tridimite appears as mosaic aggregates among plagioclase microlites, whereas glass is much more abundant in these andesites than in the older ones. A distinguishing characteristic is recognized in one of these varieties where the groundmass is formed by two kinds of glasses, one with brown color, as it appears in the rest of the lavas, and the second one with an orange tone (Fig. 5D). The mineral phases associated with each of them are the same, while contact between both glasses is sharp even on a microscopic scale; moreover, one of the glass varieties shows many large opaque microlites that are missing in the other glass. Given these features, it could be evidence of mingling processes between two melts.

MINERAL CHEMISTRY

New mineral chemistry data for Cerro de las Tórtolas Formation andesites are presented here. The studied samples are from the previously described lava flow outcrops with well-defined stratigraphic relationships and documented age: lower section lavas, representative of the Lower Miocene volcanic episode, are from La Brea and Zancarrón Cordillera, Despoblados area and Cerro de las Tórtolas and Vacas Heladas stratovolcanoes; upper section lavas, representative of the Middle Micene volcanic episode, were collected from the flows occurring at the top of these volcanoes. The location of samples is included in Table 2. Quantitative analyses were performed with a JEOL JXA-8900RWD/ED "superprobe" electron microprobe at the Cornell Center for Material Research from Cornell University (USA), with wavelength dispersive spectrometers, using 15kV accelerating voltage, 15nA beam current and 10µbeam diameter. All elements except Na were counted at least 60s (Na for 40s) for peak, and 20s for background; error is 2-5%. Standards used for calibration and data reduction include Smithsonian standards A-99 and JDF (Juan de Fuca glass) and internal standard RHA-Z. Natural mineral standards (Kakanui hornblende, PX-1 clinopyroxene, Lake County and Gary Aden plagioclases; Jarosewich *et al.*, 1980) were

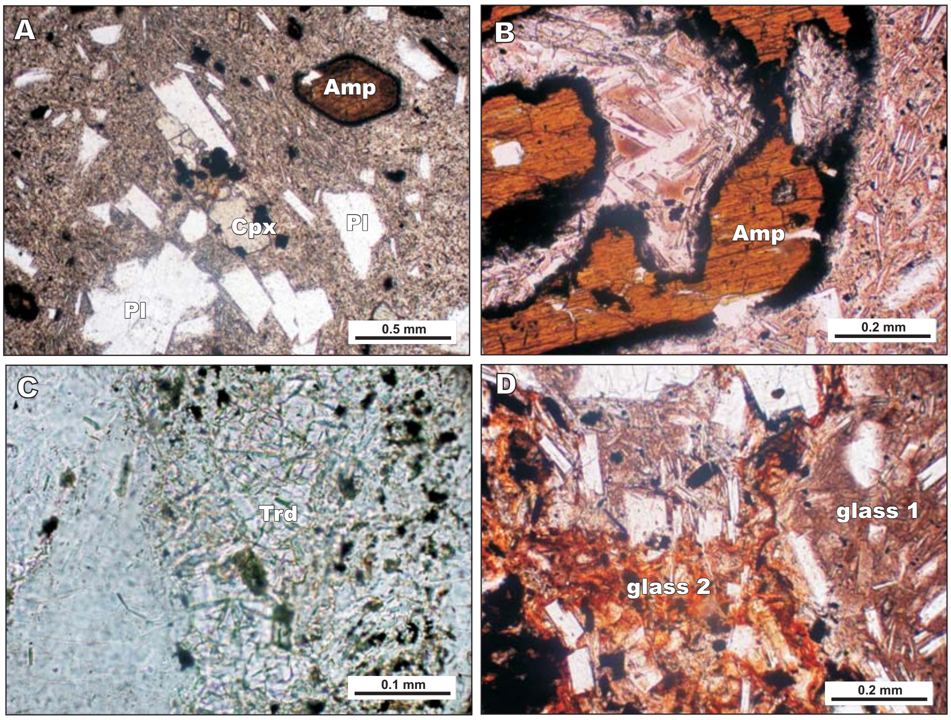

FIGURE 5. Andesites from the Middle Miocene volcanic episode of Cerro de las Tórtolas Formation: A) Porphyritic lavas with high phenocrysts/groundmass ratio; B) Amphibole with skeletal structures, coarse rim of opaque minerals and groundmass corrosion; C) Interstitial tridimite as a distinguishing feature of younger andesites; D) Two types of glasses, a brownish (glass 1) and orange one (glass 2), are recognized as part of the groundmass of the volcanic rocks.

additionally run as secondary standards during in situ mineral analyses.

The analyzed minerals were plagioclase, orthopyroxene, clinopyroxene and amphibole, according to the main paragenesis present in every sample. In all cases, measurements were performed on core and rim of selected phenocrysts in order to evaluate their composition and cristallyzation condition within the magma chambers; additionally, intermediate points between core and rim were analyzed in order to check for compositional zoning. Mineral classification and structural formulas of analyzed minerals were calculated according to the recommendations of Deer *et al.* (1992), Leake *et al.* (1997) and Morimoto (1989) for plagioclase, amphibole and pyroxene, respectively.

Plagioclase

Plagioclase phenocryst composition for the Lower Miocene andesites of the Cerro de las Tórtolas Formation is mostly labradorite to andesine (Fig. 6, Table 2). The latter corresponds to the expected variation in Ca-Na content of the feldspar crystallization and is consistent with the normal and oscillatory zoning seen under the microscope. One sample from Tórtolas Volcano and one from Despoblados show normal zoning (DI040-plg1 and SP29-plg1). Both plagioclases from Despoblados andesites show normal zoning within the bytownite. Samples from other localities however, show either reverse or oscillatory zoning. The most significant reverse zoning is seen in a particularly large phenocryst from Zancarrón (ZN162-plg2) with core and rim values of An_{60} and An_{90} respectively, and in a specimen from La Brea Cordillera SP79-plg1 with a very restricted composition within andesine. Samples with oscillatory zoning are from Tórtolas volcano and La Brea and Zancarrón Cordilleras. Those from Tórtolas volcano have values between bytownite at the rim (An_{75}, sample DI040-plg2a) and a composition close to andesine (An_{49}, DI040plg-2c) at the core. Two samples from La Brea Cordillera show oscillatory zoning but within the composition of a labradorite from rim to core (*e.g.* An_{65}, SP79-plg2a/An_{51}, SP79-plg2d) and one specimen from Zancarrón Cordillera (ZN162-plg1) has a bytownite core and oscillatory values within labradorite composition in different points towards the rim.

Samples from the Middle Miocene Cerro de las Tórtolas Formation have a labradorite composition (Fig. 6, Table 2). This composition allows us to classify petrographically these rocks as basalts, which is more consistent with their color index >40vol%, although, as will be discussed later, their chemical classification corresponds to dacites.

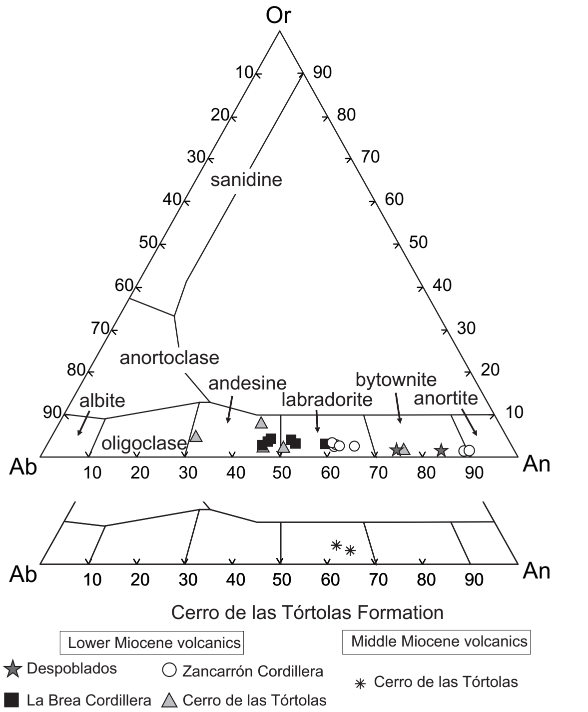

FIGURE 6. Ab-An-Or diagram that shows plagioclase phenocrysts composition from the Miocene volcanic rocks.

Orthopyroxene

Orthopyroxene from the Lower Miocene andesites is classified as enstatite in the range of En_{70} to En_{65}, without a clear zoning trend (Fig. 7A, Table 3). Most of the samples show normal zoning, although some of them present a reverse one. In both cases, the compositional zoning between core and rim differs in less than 0.5%. For example, sample ZN162-opx1 from Zancarrón Cordillera shows a reverse zoning between $En_{66.0}$ to $En_{66.3}$ whereas sample SP29-opx1 from Despoblados shows normal zoning between $En_{66.69}$ to $En_{66.26}$. Only the two analyzed phenocrysts from La Brea Cordillera (SP79-opx1 and opx2) exhibit a more significant reverse zoning also recognizable under the microscope, with variation of En content between rims and core of more than 5%. CaO values are low, between 0.5 to 1wt.%, as expected for orthopyroxenes, although phenocrysts from Despoblados show a generally higher CaO content (1.3wt.%). The highest value was measured in the core of one crystal from Zancarrón (ZN162-opx3c, 1.75wt.% CaO), and variable contents were detected in a crystal from Tórtolas volcano (DI040-opx2, 0.49wt.% CaO at the core, and 0.71wt.% at the rim).

Phenocrysts for the samples of the Middle Miocene volcanic episode are enstatites with an average composition of En_{69} (Fig. 7A; Table 3) and a relative homogeneous composition between measured points. One of the samples (MQ28-opx1) shows a sligthy normal zoning with values between En_{68} to En_{67} from core to rim. Sample MQ28-opx2 shows an incipient reverse zoning between En_{68} to En_{71}.

Clinopyroxene

The average clinopyroxene phenocrysts from the Lower Miocene andesites are augites with Wo_{42} Fs_{16} En_{41} proportion (Fig. 7B; Table 4). There is a moderate dispersion of the data around the average value, although clinopyroxene from Zancarrón shows a more evolved Fe-rich composition (Fs_{19}) relative to the Depoblados, Cerro de las Tórtolas volcano and La Brea areas (Fs_{15}-Fs_{16}). The composition of cores and rims is relatively homogeneous. An intermediate point in two samples (SP29-cpx2b from Despoblados and ZN162-cpx2b from Zancarrón) shows enrichment in Mg in relation both to the rim and the core that evidences incipient oscillatory zoning.

TABLE 2. Representative microprobe analyses of plagioclase phenocrysts from the Lower and Middle Miocene volcanic episodes of the Cerro de las Tórtolas Formation (Lower and Upper Sections of the unit). (Structural formula is based on 8 oxygens and 5 cations; a. b. c. etc. indicate points from rim to core)

Unit	Cerro de las Tórtolas Formation - Lower Section																				Upper Section	
Locality	Tórtolas volcano					Zancarrón Cordillera							La Brea Cordillera						Despoblados		Tórtolas volcano	
Coordinates	29°57'48"S / 69°50'05"W					29°36'49"S / 69°46'60"W							29°43'45"S / 69°41'53"W						29°30'57"S / 69°45'57"W		29°56'36"S / 69°51'22"W	
Sample	DI040	DI040	DI040	DI040	DI040	ZN162	ZN162	ZN162	ZN162	ZN162	ZN162	ZN162	SP79	SP79	SP79	SP79	SP79	SP79	SP29	SP29	MQ28	MQ28
Crystal	plg-1a	plg-1b	plg-2a	plg-2b	plg-2c	plg-1a	plg-1b	plg-1c	plg-1d	plg-2a	plg-2b	plg-2c	plg-1a	plg-1b	plg-2a	plg-2b	plg-2c	plg-2d	plg-1a	plg-1b	plg-1b	plg-2a
SiO_2	67.31	57.92	49.9	63.58	56.45	52.93	54.27	46.13	45.94	52.18	53.52	53.9	57.55	57.58	52.27	55.67	54.18	55.91	50.23	47.78	55.82	55.87
TiO_2	0	0.03	0.03	0.26	0.04	0.06	0.06	0.02	0.03	0.04	0.05	0.02	0.03	0.02	0.04	0.03	0.05	0.02	0.02	0.03	0.04	0.02
Al_2O_3	23.48	27.17	32.15	22.26	27.9	29.52	29.21	34.6	34.53	30.09	29.47	29.39	26.72	26.88	30.4	27.35	29.2	28.12	32.07	33.82	28.49	28.33
FeO	0.12	0.27	0.62	1.27	0.36	0.6	0.63	0.49	0.53	0.55	0.56	0.6	0.38	0.43	0.54	0.41	0.47	0.45	0.51	0.54	0.48	0.47
MnO	0	0	0	0	0	0	0	0	0	0	0	0	0	0	0	0	0	0	0	0.03	0.02	0
MgO	0	0	0	0	0	0	0	0	0	0	0	0	0	0	0	0	0	0	0.05	0.05	0.07	0.03
CaO	4.2	9.45	15.52	6.75	10.37	12.47	12.24	18.44	18.15	13.42	12.54	12.45	9.35	9.32	13.55	10.21	11.94	10.75	15.38	17.35	10.94	10.7
Na_2O	4.99	5.97	2.78	4.41	5.59	4.29	4.29	1.19	1.36	3.93	4.16	4.41	5.55	5.65	3.69	5.14	4.52	5.21	2.78	1.88	5.26	5.21
K_2O	0.52	0.4	0.1	1.04	0.33	0.4	0.43	0.06	0.07	0.33	0.38	0.41	0.71	0.65	0.32	0.54	0.39	0.53	0.13	0.07	0.32	0.37
Total	100.62	101.21	101.1	99.57	101.04	100.27	101.13	100.93	100.61	100.54	100.68	101.18	100.29	100.53	100.81	99.35	100.75	100.99	101.18	101.56	101.44	101
Si	2.9	2.57	2.26	2.82	2.52	2.4	2.43	2.11	2.11	2.37	2.41	2.42	2.58	2.57	2.36	2.53	2.44	2.5	2.27	2.17	2.49	2.5
Al	1.19	1.42	1.72	1.17	1.47	1.58	1.54	1.87	1.87	1.61	1.57	1.56	1.41	1.42	1.62	1.46	1.55	1.48	1.71	1.81	1.5	1.49
Ca	0.19	0.45	0.75	0.32	0.5	0.61	0.59	0.9	0.89	0.65	0.61	0.6	0.45	0.45	0.66	0.5	0.58	0.52	0.75	0.84	0.52	0.51
Na	0.42	0.51	0.24	0.38	0.48	0.38	0.37	0.11	0.12	0.35	0.36	0.38	0.48	0.49	0.32	0.45	0.39	0.45	0.24	0.17	0.45	0.45
K	0.03	0.02	0.01	0.06	0.02	0.02	0.02	0	0	0.02	0.02	0.02	0.04	0.04	0.02	0.03	0.02	0.03	0.01	0	0.02	0.02
Ab	65.2	52.11	24.34	49.97	48.45	37.49	37.84	10.42	11.89	33.99	36.68	38.15	49.62	50.32	32.4	46.15	39.74	45.31	24.46	16.33	45.67	45.84
An	30.33	45.59	75.09	42.27	49.67	60.21	59.66	89.23	87.71	64.14	61.11	59.52	46.2	45.87	65.75	50.66	58.01	51.66	74.79	83.27	52.5	52.02
Or	4.47	2.3	0.58	7.75	1.88	2.3	2.5	0.35	0.4	1.88	2.2	2.33	4.18	3.81	1.85	3.19	2.26	3.03	0.75	0.4	1.83	2.14

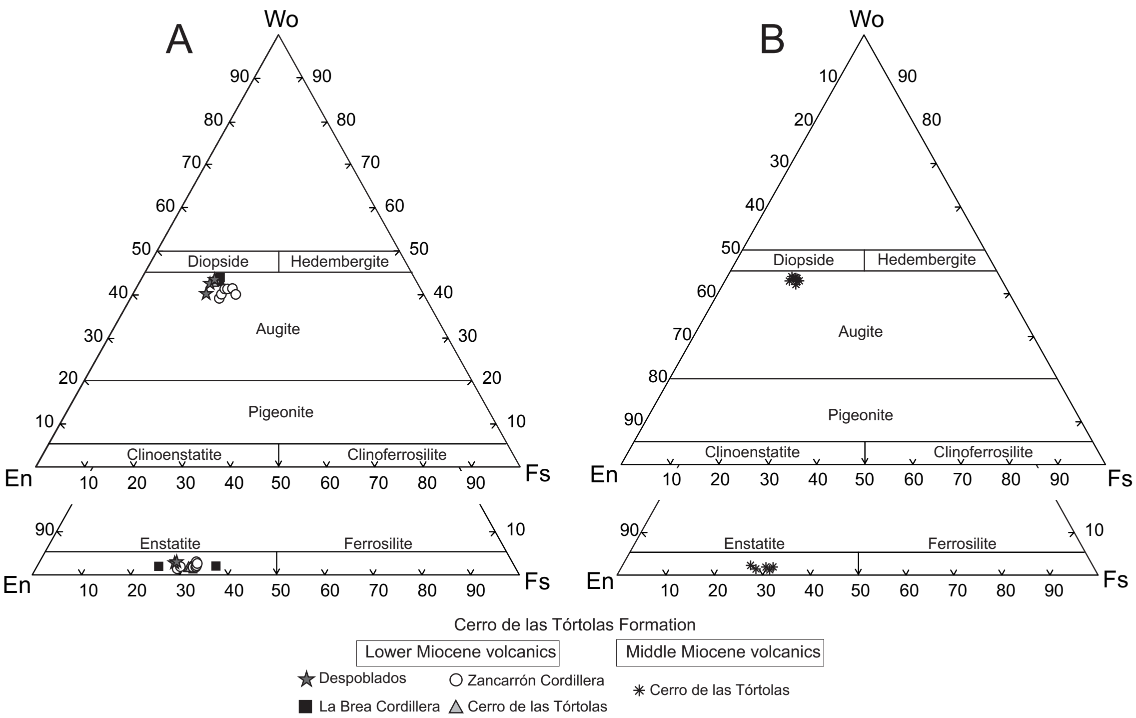

FIGURE 7. Diagrams of composition ranges of orthopyroxene and clinopyroxene (both according to Morimoto, 1989), from A) Lower Miocene volcanic rocks; B) Middle Miocene volcanic rocks.

Clinopyroxene from the Middle Miocene andesitic volcanic rocks is an augite of Wo_{43} En_{43} Fs_{14} composition (Fig. 7B; Table 4).

Amphibole

Amphibole is the least common mafic mineral in the Lower Miocene samples from the Cerro de las Tórtolas Formation, where it is only present as phenocrysts in the andesites of Cerro de las Tórtolas volcano and in the Despoblados area. Phenocrysts are classified as pargasites (Table 5; Fig. 8). Three measured points, one corresponding to a sample from Cerro de la Tórtolas volcano (DI0410-anf2b) and two from a sample from Despoblados (SP29anf-3a and 3b) show relatively low values of SiO_2 and high values of Al_2O_3. These phenocrysts are larger than the rest of the analyzed amphiboles (Fig. 8). Their formation is probably related to an early stage of nucleation, which could explain their low content in silica.

Amphiboles from the Middle Miocene andesites are also classified as calcic, belonging to the pargasite group (Table 5; Fig. 8), which is the expected composition for amphiboles of a calc-alkaline magma. The Al_2O_3 and SiO_2

TABLE 3. Representative microprobe analyses of orthopyroxene phenocrysts from the Lower and Middle Miocene volcanic episodes of the Cerro de las Tórtolas Formation (Lower and Upper Sections of the unit). (Structural formula is based on 6 oxygens and 4 cations; a. b. c. etc. indicate points from rim to core)

Unit	Cerro de las Tórtolas Formation - Lower Section															Upper Section				
Locality	Tórtolas volcano		Zancarrón Cordillera							La Brea Cordillera				Despoblados		Tórtolas volcano				
Sample	DI040	DI040	ZN162	ZN162	ZN162	ZN162	ZN162	ZN162	ZN162	SP79	SP79	SP79	SP79	SP29	SP29	MQ28	MQ28	MQ28	MQ28	MQ28
Crystal	opx-2a	opx-2b	opx-1a	opx-1b	opx-2a	opx-2b	opx-3a	opx-3b	opx-3c	opx-1a	opx-1b	opx-2a	opx-2b	opx-1a	opx-1b	opx-1a	opx-1b	opx-2a	opx-2b	opx-2c
SiO_2	53.85	53.7	52.81	53.06	53.35	52.98	52.98	53.09	52.83	53.73	52.67	54.67	53.71	53.95	54.28	53.87	53.92	54.7	54.05	53.38
TiO_2	0.1	0.11	0.21	0.19	0.19	0.17	0.2	0.19	0.33	0.11	0.11	0.14	0.14	0.25	0.2	0.16	0.18	0.26	0.18	0.14
Al_2O_3	0.89	1.22	1.75	1.71	1.43	1.64	1.33	1.28	1.33	0.73	0.77	0.73	0.86	1.04	0.75	0.94	1.18	1.01	1.31	1.69
FeO	19.14	19.21	19.99	20.03	18.42	18.17	20.04	20.39	20.21	20.54	23.03	16.11	20.65	18.08	17.81	19.62	18.89	16.84	17.83	19.44
MnO	1.14	1.46	0.49	0.49	0.54	0.49	0.59	0.57	0.57	0.74	0.68	0.47	0.69	0.81	0.83	0.94	0.82	0.55	0.73	0.74
MgO	24.46	24.82	24	23.82	25.07	25.48	23.58	23.9	23.82	24.28	22.21	27.27	24.05	25.89	26.24	24.55	24.99	25.99	26.03	24.73
CaO	0.71	0.49	1.03	1.03	0.98	0.89	0.96	1.15	1.73	0.74	0.83	0.94	0.79	1.23	1.32	0.98	1.04	1.15	0.73	0.4
Na_2O	0.04	0.01	0.03	0.04	0.01	0	0.03	0.01	0.05	0.01	0.02	0	0	0.04	0.01	0.01	0.02	0.04	0.01	0.02
K_2O	0.01	0	0	0	0	0	0	0	0	0	0	0.01	0	0	0	0.01	0	0.01	0	0
Total	100.34	101.02	100.31	100.37	99.99	99.82	99.71	100.58	100.87	100.88	100.32	100.34	100.89	101.28	101.42	101.08	101.04	100.55	100.87	100.54
Si	1.971	1.952	1.936	1.946	1.949	1.934	1.959	1.945	1.930	1.963	1.959	1.967	1.967	1.941	1.948	1.959	1.955	1.976	1.950	1.946
Al^{IV}	0.029	0.048	0.064	0.054	0.051	0.066	0.041	0.055	0.057	0.031	0.034	0.031	0.032	0.044	0.032	0.040	0.045	0.024	0.050	0.054
Al^{VI}	0.010	0.004	0.012	0.020	0.011	0.004	0.017	0.001	0.000	0.000	0.000	0.000	0.000	0.000	0.000	0.000	0.005	0.020	0.006	0.019
Fe^{2+}	0.569	0.545	0.570	0.588	0.533	0.502	0.604	0.581	0.549	0.590	0.673	0.457	0.605	0.482	0.472	0.563	0.541	0.509	0.503	0.565
Fe^{3+}	0.017	0.039	0.043	0.027	0.030	0.053	0.016	0.044	0.068	0.037	0.043	0.028	0.027	0.062	0.062	0.034	0.032	0.000	0.035	0.028
Mg	1.335	1.245	1.312	1.302	1.365	1.386	1.300	1.306	1.297	1.322	1.232	1.463	1.313	1.389	1.404	1.331	1.350	1.400	1.400	1.344
Mn	0.035	0.045	0.015	0.015	0.017	0.015	0.018	0.018	0.018	0.023	0.021	0.014	0.021	0.025	0.025	0.029	0.025	0.017	0.022	0.023
Ca	0.028	0.019	0.040	0.040	0.038	0.035	0.038	0.045	0.068	0.029	0.033	0.036	0.031	0.047	0.051	0.038	0.040	0.045	0.28	0.016
Wo	1.40	0.95	2.0	2.1	1.9	1.8	1.9	2.3	3.4	1.44	1.65	1.81	1.55	2.36	2.52	1.91	2.03	2.26	1.41	0.79
En	67.27	67.48	66.3	66.0	68.8	69.6	65.8	65.5	64.8	66.05	61.50	73.20	65.71	69.26	69.69	66.71	67.90	71.05	70.40	68.04
Fs	31.31	31.55	31.7	31.9	29.3	28.6	323	32.2	31.8	32.49	36.84	25.98	32.72	28.36	27.79	31.36	30.06	26.68	28.17	31.16

content are very homogenous in the analyzed crystals with no significant variation between the core and rim. There is only one specimen, MQ28-anf2a, that differs from the rest due to its anomalous lower value of Al_2O_3 (9.11wt.%) and higher value of SiO_2 (46.63wt.%). The rim of the phenocryst also shows the lowest MgO content (10.06wt.%) and highest FeO (15.25wt.%) being classified as edenite (Fig. 8).

CHEMISTRY OF MIOCENE VOLCANISM

Geochemical data of volcanic samples representative of the Miocene Cerro de Las Tórtolas Formation were largely discussed in a previous work in the context of the geochemical evolution of Tertiary magmatism over the Pampean flat slab (Kay *et al*., 1987, 1991, 1999; Bissig *et al*., 2003; Litvak *et al*., 2007). However, a brief description of the main features regarding major, trace, rare earth elements and isotopic data is included below for further discussion on the petrogenesis of this volcanism.

The main focus is the difference in chemical composition between the two volcanic episodes of the Miocene Cerro de las Tórtolas Formation. According to the K_2O vs. SiO_2 diagram, the older Miocene lavas are andesites to dacites with 55-63wt.% SiO_2; whereas the younger lavas are mainly dacites and ryholites, with a SiO_2 range of 63-71wt.% (Fig. 9A). The TAS diagram clearly shows that Middle to Upper Miocene lavas are mainly dacites and only two samples are classified as ryholites (Fig. 9B). The samples with the highest silica content come from the dacitic tuffs included as part of the Middle Miocene volcanic rocks of the region. Despite the fact that both sections are petrographically classified as andesites, the Lower Miocene lavas are andesites according to their chemistry and the Middle Miocene lavas are dacites (Fig. 9A, B). They all are medium to high K lavas, with a calc-alkaline signature according to their ratio SiO_2 vs. FeO/Mg (Fig. 9C).

The Miocene lavas of the Cerro de las Tórtolas in the Valle del Cura show typical arc-type trace element patterns on chondrite or mantle normalized trace element plots, as noted by previous authors (Kay *et al*., 1987, 1991, 1999; Ramos *et al*., 1989; Otamendi *et al*., 1994; Bissig *et al*., 2003; Litvak *et al*., 2007). Overall, the reported La/Ta ratios of 22–35 for these Miocene magmas are indicative of arc mantle sources, whereas the high Ba/Ta ratios for the sequences also reflect an arc-type origin. This is also seen in the Ba/La ratios >20, where older lavas show relatively higher Ba/La ratios than the younger lavas (Fig. 9D). As pointed out, trace elements ratios of Middle to Upper Miocene dacites show a more evolved arc-related signature than the Lower to Middle Miocene andesites (Kay *et al*., 1991, 1999; Litvak *et al*., 2007).

In general, REE ratios of these Miocene lavas show a moderate slope of LREE relative to HREE on a chondrite normalized diagram (Bissig *et al*., 2003; Kay *et al*., 1991; 1999; Litvak *et al*., 2007). However, a significant difference is seen within the Cerro the las Tórtolas Formation when considering in detail La/Sm, La/Yb and Sm/Yb ratios for the two sections of the unit (Fig. 10A, B). Lower andesite section from the Lower Miocene volcanic episode shows values of La/Sm between 2 and 4.5, while upper andesite section of Middle Miocene age shows values between 3 and 7.5, reflecting the fractionation of different residual mineral phases left at variable crustal depths during

TABLE 4. Representative microprobe analyses of clinopyroxene phenocrysts from the Lower and Middle Miocene volcanic episodes of the Cerro de las Tórtolas Formation (Lower and Upper Sections of the unit). (Structural formula is based on 6 oxygens and 4 cations; a. b. c. etc. indicate points from rim to core)

Unit	Cerro de las Tórtolas Formation - Lower Section									
Locality	Tórtolas volcano		Zancarrón Cordillera						Brea Cordillera	
Sample	DI040	DI040	ZN162	ZN162	ZN162	ZN162	ZN162	ZN162	SP79	SP79
Crystal	cpx-2a	cpx-2b	cpx-1a	cpx-1b	cpx-2a	cpx-2b	cpx-3a	cpx-3b	cpx-1a	cpx-2b
SiO_2	52.53	51.9	51.55	50.82	50.81	51.3	50.62	50.86	51.63	52.18
TiO_2	0.35	0.47	0.56	0.65	0.8	0.68	0.63	0.64	0.33	0.32
Al_2O_3	1.68	2.38	1.9	2.52	3.36	2.51	2.24	2.36	1.63	1.43
FeO	9.25	9.34	11.32	11.49	11.24	10.91	12.01	12.58	9.84	9.91
MnO	0.57	0.49	0.4	0.43	0.35	0.31	0.39	0.38	0.35	0.38
MgO	15.02	14.58	14.92	14.08	14.21	15.12	13.74	13.87	14.35	14.55
CaO	21.34	21.24	19.55	20.55	19.97	19.45	19.72	19.51	21.8	21.69
Na_2O	0.36	0.44	0.3	0.37	0.36	0.36	0.33	0.32	0.35	0.34
K_2O	0.01	0	0	0	0.01	0	0.02	0	0	0.01
Total	101.11	100.84	100.5	100.91	101.11	100.64	99.7	100.52	100.28	100.81
Si	1.928	1.922	1.913	1.883	1.876	1.896	1.903	1.898	1.971	1.927
Al^4	0.072	0.071	0.083	0.11	0.124	0.104	0.097	0.102	0.071	0.062
Al^6	0.001	0	0	0	0.022	0.005	0.003	0.002	0	0
Fe^{2+}	0.207	0.213	0.27	0.241	0.263	0.25	0.294	0.306	0.203	0.215
Fe^{3+}	0.077	0.092	0.081	0.115	0.084	0.087	0.084	0.087	0.102	0.091
Mg	0.822	0.792	0.825	0.778	0.782	0.833	0.77	0.0772	0.794	0.801
Mn	0.018	0.011	0.013	0.013	0.011	0.01	0.012	0.012	0.011	0.012
Ca	0.839	0.865	0.777	0.816	0.79	0.77	0.794	0.78	0.867	0.858
Wo	42.76	43.17	39.53	41.56	40.93	39.5	40.65	39.98	43.85	43.51
En	41.87	41.23	41.97	39.62	40.52	42.72	39.4	39.44	40.15	40.51
Fs	15.37	15.6	18.5	18.83	18.55	17.79	19.96	20.68	16	16.08

Unit	Cerro de las Tórtolas Formation - Lower Section				Upper Section							
Locality	Despoblados				Tortolas volcano							
Sample	SP29	SP29	SP29	SP29	MQ28	MQ28	MQ28	MQ28	MQ28	MQ28	MQ28	MQ28
Crystal	cpx-1a	cpx-2a	cpx-2b	cpx-2c	cpx-1a	cps-b	cpx-2a	cpx-2b	cpx-2c	cpx-3a	cpx-3b	cpx-3c
SiO_2	51.64	52.01	52.74	51.16	52.51	52.46	52.49	51.05	50.85	52.35	52.2	52.39
TiO_2	0.55	0.46	0.46	0.73	0.46	0.5	0.45	0.89	0.82	0.52	0.45	0.47
Al_2O_3	2.55	2.07	1.41	2.84	1.74	1.88	1.83	3.16	3.49	2.03	1.89	1.77
FeO	8.96	9.09	9.24	9.25	8.44	8.16	8.28	8.96	9.23	8.7	8.38	7.86
MnO	0.36	0.4	0.44	0.41	0.31	0.3	0.32	0.38	0.43	0.32	0.33	0.29
MgO	15	15.39	16.34	15.3	15.58	15.5	15.53	15.35	14.62	15.13	15.39	15.46
CaO	21.38	20.88	20.03	20.98	21.59	21.42	21.3	20.47	20.7	21.57	21.68	21.81
Na_2O	0.39	0.37	0.26	0.36	0.43	0.38	0.42	0.38	0.44	0.47	0.4	0.41
K_2O	0	0.01	0	0	0.01	0	0	0.01	0	0	0	0
Total	100.83	100.68	100.92	101.03	101.07	100.6	100.62	100.65	100.58	101.09	100.72	100.46
Si	1.897	1.912	1.932	1.875	1.919	1.926	1.927	1.876	1.875	1.917	1.916	1.925
Al^4	0.103	0.088	0.061	0.123	0.075	0.074	0.073	0.124	0.125	0.083	0.082	0.075
Al^6	0.007	0.002	0	0	0	0.008	0.006	0.013	0.026	0.004	0	0.002
Fe^{2+}	0.182	0.193	0.216	0.171	0.166	0.185	0.182	0.187	0.2	0.182	0.166	0.165
Fe^{3+}	0.093	0.087	0.068	0.112	0.092	0.065	0.072	0.089	0.085	0.084	0.091	0.076
Mg	0.821	0.844	0.892	0.836	0.849	0.849	0.85	0.841	0.0804	0.826	0.842	0.847
Mn	0.011	0.012	0.014	0.013	0.01	0.009	0.01	0.012	0.013	0.01	0.01	0.009
Ca	0.842	0.823	0.786	0.824	0.846	0.843	0.838	0.806	0.818	0.846	0.852	0.859
Wo	43.17	42.01	39.8	42.12	43.1	43.19	42.93	41.67	42.06	43.43	43.45	43.9
En	42.14	43.08	45.17	42.73	43.27	43.48	43.54	43.47	41.86	42.38	42.91	43.29
Fs	14.7	14.91	15.02	15.15	13.64	13.32	13.53	14.85	15.53	14.18	13.63	12.81

TABLE 5. Representative microprobe analyses of amphibole phenocrysts from the Lower and Middle Miocene volcanic episodes of the Cerro de las Tórtolas Formation (Lower and Upper Sections of the unit). (Structural formula is based on 23 oxygens and 15 cations; a. b. c. etc. indicate points from rim to core)

Unit	Cerro de las Tórtolas Formation: Lower Section									Upper Section				
Locality	Tortolas volcano			La Brea Cordillera						Tórtolas volcano				
Sample	DI040	DI040	DI040	SP29	SP29	SP29	SP29	SP29	SP29	MQ28	MQ28	MQ28	MQ28	MQ28
Specimen	anf-1a	anf-1b	anf-2b	anf-1a	anf-1b	anf-2a	anf-2b	anf-3a	anf-3b	anf-1a	anf-1b	anf-2a	anf-2b	anf-2c
SiO_2	43.63	43.28	41.93	43.32	43.16	42.87	42.97	41.6	41.87	43.12	43.80	46.63	42.86	43.26
TiO_2	3.27	2.66	3.21	3.23	3.36	2.88	2.90	2.79	2.80	3.04	23.60	4.27	2.83	2.68
Al_2O_3	11	11.52	13.26	11.34	11.14	11.64	11.75	13.29	13.09	11.25	11.65	9.11	12.13	11.98
FeO	12.69	12.83	12.11	13.29	12.54	12.94	12.81	11.88	11.92	12.87	9.82	15.25	11.23	10.49
MnO	0.36	0.3	0.23	0.29	0.25	0.23	0.20	0.13	0.12	0.13	0.10	0.27	0.09	0.12
MgO	14.08	14.34	13.69	13.94	14.21	14.19	14.24	14.17	14.32	13.88	15.90	10.06	14.83	15.50
CaO	11.65	11.54	11.73	11.65	11.58	11.69	11.58	12.12	12.13	11.59	11.97	13.24	11.61	11.58
Na_2O	2.39	2.29	2.54	2.25	2.40	2.28	2.3	2.38	2.31	2.48	2.44	0.14	2.51	2.45
K_2O	0.71	0.62	0.66	0.65	0.66	0.59	0.59	0.68	0.65	0.74	0.63	0.24	0.67	0.64
Total	99.78	99.38	99.36	99.96	99.3	99.31	99.34	99.04	99.21	99.10	98.91	100.77	98.76	98.7
Si	6.32	6.27	6.09	6.26	6.28	6.22	6.23	6.03	6.05	6.29	6.30	6.71	6.22	6.25
Al^{IV}	1.68	1.73	1.91	1.74	1.72	1.78	1.77	1.97	1.95	1.71	1.70	1.29	1.78	1.75
Al^{VI}	0.20	0.23	0.36	0.20	0.19	0.21	0.23	0.30	0.28	0.23	0.27	0.26	0.30	0.29
Ti	0.36	0.29	0.35	0.35	0.37	0.31	0.32	0.30	0.30	0.33	0.28	0.46	0.31	0.29
Fe^{2+}	1.54	1.39	1.46	1.52	1.53	1.37	1.40	1.17	1.14	1.57	1.11	1.84	1.34	1.08
Fe^{3+}	0.00	0.16	0.01	0.09	0.00	0.20	0.15	0.27	0.30	0.00	0.07	0.00	0.03	0.18
Mg	3.04	3.10	2.96	3.00	3.03	3.07	3.08	3.06	3.08	3.02	3.41	2.16	3.21	3.34
Mn	0.04	0.04	0.03	0.04	0.03	0.03	0.02	0.02	0.01	0.02	0.01	0.00	0.01	0.01
Ca	1.81	1.79	1.83	1.80	1.81	1.82	1.80	1.88	1.88	1.81	1.84	2.00	1.81	1.79
Na	0.67	0.64	0.72	0.63	0.68	0.64	0.65	0.67	0.65	0.70	0.68	0.47	0.71	0.69
K	0.13	0.11	0.12	0.12	0.12	0.11	0.11	0.13	0.12	0.14	0.12	0.04	0.12	0.12

magma equilibration. In the older lavas, trace element inferred that the residual assemblage is dominated by amphibole and pyroxene, whereas in the younger lavas it is dominated by garnet. Mass balance calculations and trace elements in the melting models made on Cerro de las Tórtolas rocks evidenced the mineralogical changes in the Miocene magmas and provided a quantitative guide to the residual mineralogy (Kay *et al*. (1987, 1991). As a result, these authors concluded that the addition of garnet to the fractionation of Middle Miocene magmas could generate the steep and variable REE patterns and that the phenocrysts of the younger lavas from the Cerro de las Tórtolas crystallized from a melt that had been in equilibrium with garnet, which reflects higher pressure conditions for magma equilibration.

Eu anomalies are also useful for evaluating pressure conditions. The coexistence of high La/Yb ratios, low La/Sr ratios and little or no Eu anomalies corroborate less plagioclase fractionation, which means high pressure conditions for that particular assemblage (Kay *et al*., 1991). The relationship between Sr and LREE contents as expressed by the La/Sr ratio, the steepness of the REE pattern as expressed by chondrite-normalized La/Yb ratios and the Eu anomaly (Eu/Eu*) can be seen in Figure 10C, D. The main change in the chemical trend of the Miocene volcanism is indicated by a decrease in plagioclase fractionation. This occurs in the Middle Miocene volcanic episode of the Cerro de las Tórtolas Formation, showing the highest La/Yb ratios with smaller Eu anomalies than in the older lavas (Kay *et al*., 1991; Litvak *et al*., 2007). Positive Eu anomalies from the youngest Cerro de las Tórtolas rocks may suggest high level crystal fractionation, as they contain plagioclase and amphibole phenocrysts as pointed out by Kay *et al*. (1987, 1991).

Nd and Sr isotope ratios show that Cerro de las Tórtolas volcanic rocks are more enriched in radiogenic Sr than the older Tertiary volcanic rocks from the Pampean flat slab, at 30°S, suggesting a higher contribution of crustal derived material (Fig. 11).

ESTIMATION OF P-T CONDITIONS

A number of geobarothermometers were applied to the Miocene lavas of Cerro de las Tórtolas. Separate

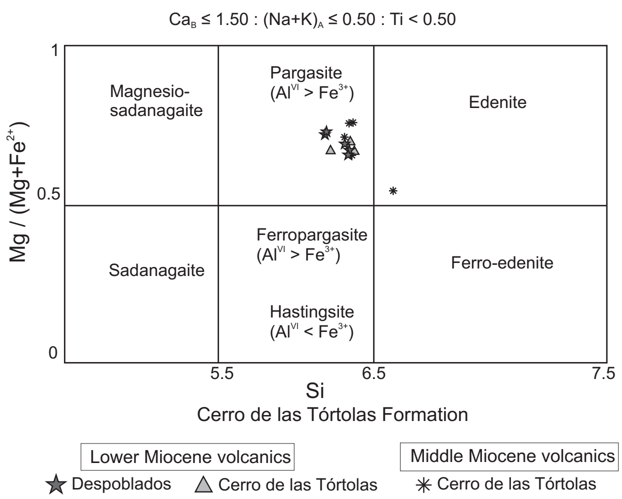

FIGURE 8. Classification diagram of amphibole phenocrysts from the Miocene volcanic rocks, according to Leake *et al*. (1997).

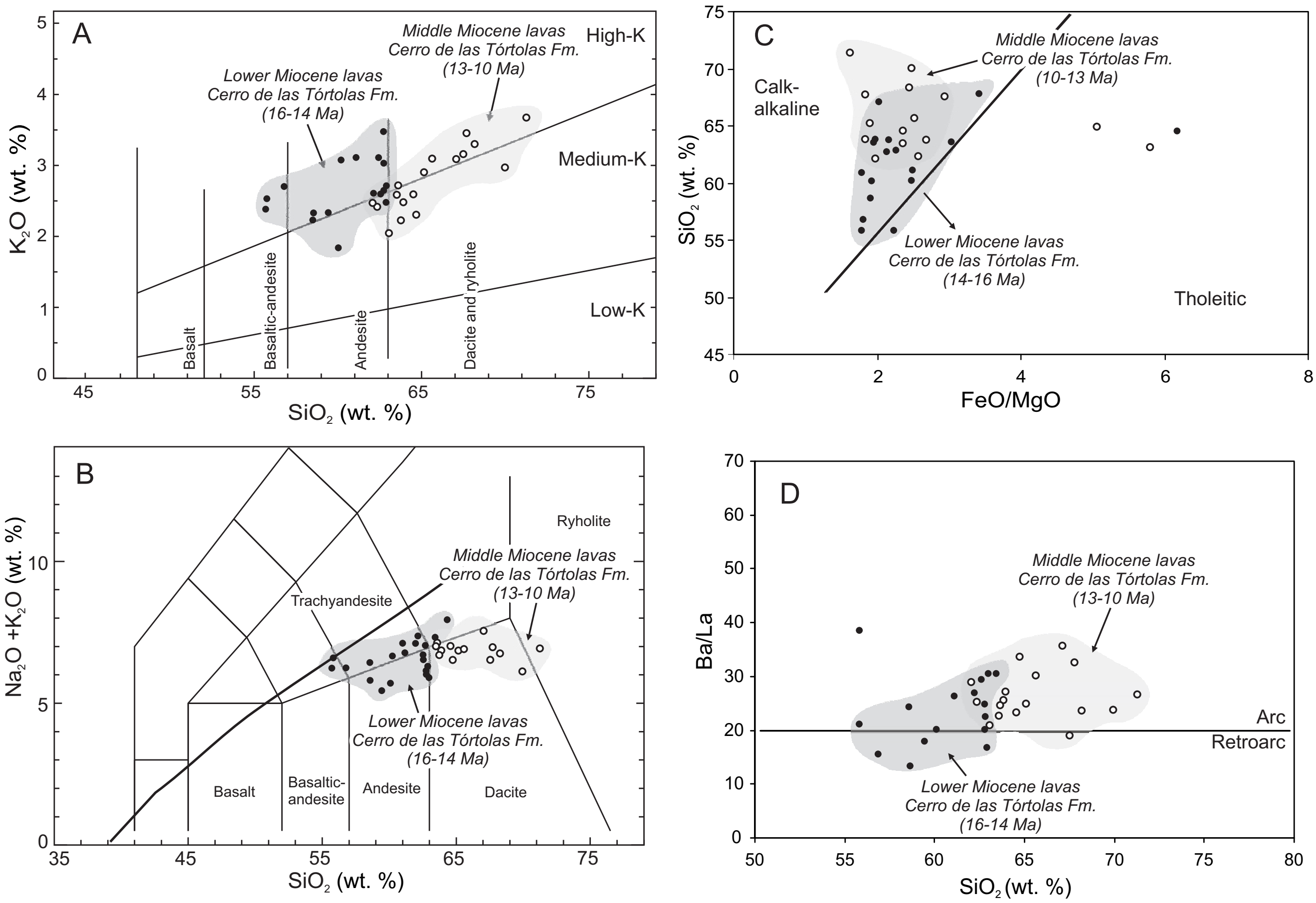

FIGURE 9. Geochemistry of Cerro de las Tórtolas Formation: A) K_2O vs. SiO_2 showing the medium to high K signature (Peccerillo and Taylor, 1976); B) TAS (Total Alkaline vs. Silica) classification (Le Maitre *et al.*, 1989) and the calc-alkaline/alkaline division of Irving and Baragar (1971) showing the two groups of lavas: a mostly andesitic one and another, mainly dacitic; C) SiO_2 vs. FeO/MgO ratio for the Miocene lavas with the tholeiitic and calk-alkaline field of Myashiro (1974); D) Ba/La vs. SiO_2 showing the arc-like signature of the lavas; boundary between arc and back arc is from Kay and Gordillo (1994). Compilation of chemical data for the Miocene volcanism cames from Kay *et al.* (1987, 1988, 1991, 1999), Bissig *et al.* (2003) and Litvak *et al.* (2007).

compositions, both from the rim and core, were considered in order to evaluate a potential variation of P and T conditions during crystallization (Table 6 and 7).

Equilibrium pressure was estimated, at first, through classical Al-in amphibole geobarometers (Hollister *et al.*, 1987; Johnson and Rutherford, 1989; Schmidt, 1992). We selected samples that contained amphibole in their mode (DI040, SP29 for the lower section and MQ28 for the upper section of the Cerro de las Tórtolas Formation). These Al-in amphibole geobarometers were applied in order to obtain a general overview of pressure conditions in the magmatic chamber where the phenocrysts were formed, although the studied rocks do not contain the typical equilibrium mineral assemblage required to use this geobarometer (hornblende + biotite + plagioclase + quartz + orthoclase + sphene + ilmenite/magnetite). Results show pressure values between 7 and 6kb for both sections when applying the Hollister *et al.* (1987) and Schmidt (1992) methods. In comparison, the Johnson and Rutherford (1989) geobarometer gives 1kb lower results, from 6 to 5kb. Ridolfi *et al.* (2010) algorithms, based on amphibole composition in arc-related volcanic rock, were also applied. The results show the lowest P values of the studied sequences with P ranging from 4 to 3kb (Table 7).

Temperature conditions were estimated according to different methods. The prerequisite of thermometry, an assumption of chemical equilibrium among the mineral phases, is well justified in most of the studied samples. However, there are some samples with reverse zoning in which the application of geothermometers were not consistent with the rest of the samples.

In particular, two-pyroxene geothermometers, such as Brey and Kholer (1990), Fonarev and Graphchikov (1991), Lindlsey and Frost (1992) and Putirka (2008) are very useful and were also applied in studies of volcanic rocks. In general, pyroxene phenocrysts are compositionally quite homogeneous, despite the two specimens of orthopyroxene

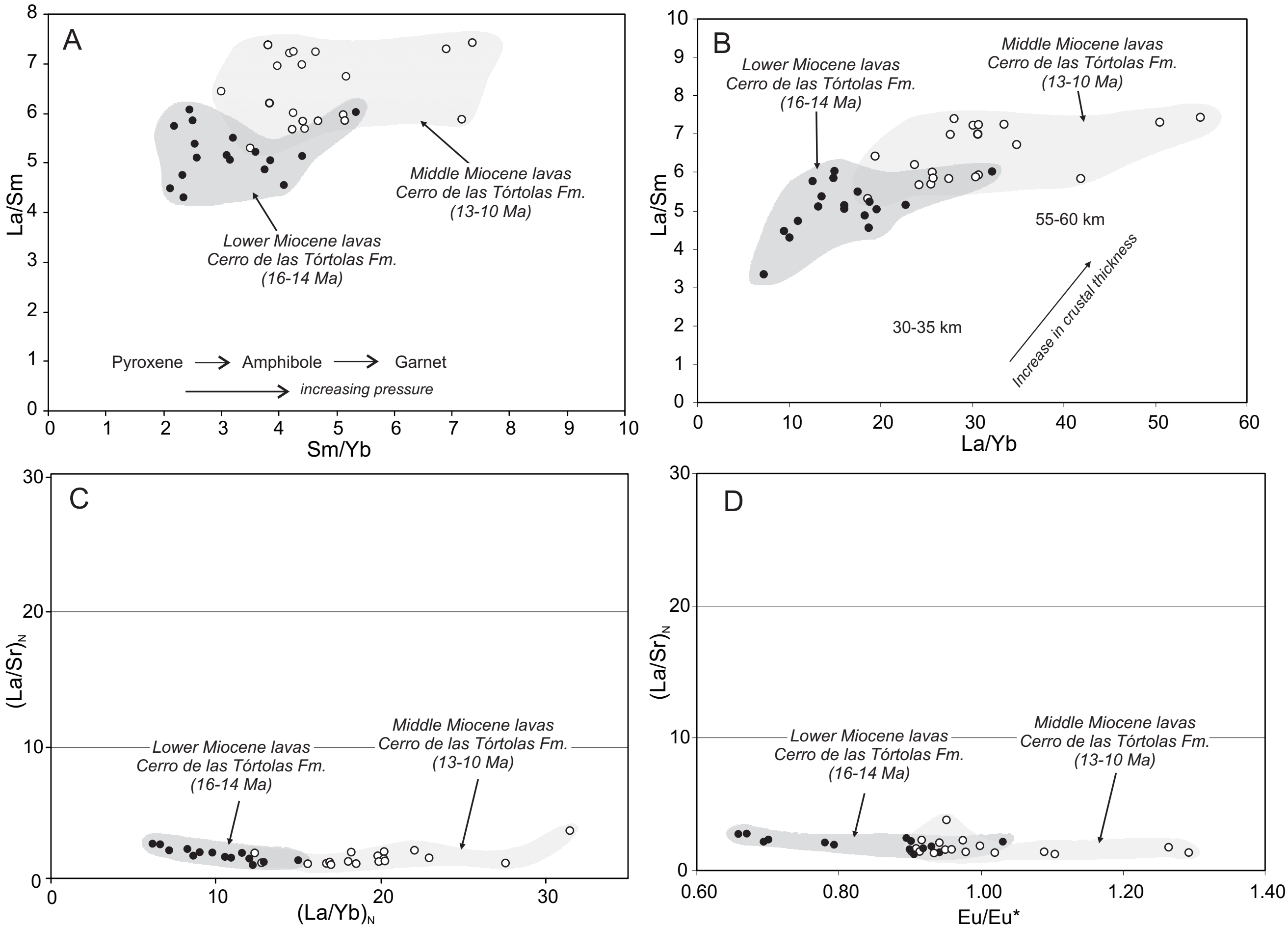

FIGURE 10. A) La/Sm vs. Sm/Yb ratios for Miocene lavas indicate amphibole and pyroxene as residual mineral assemblages for the Lower to Middle Miocene lavas, while the Middle to Upper Miocene assemblage is dominated by garnet; B) REE ratios suggest a deeper site of magma equilibration for the arc-related younger lavas due to a thicker crust; C) $(La/Sr)_N$ vs. (La/Yb) ratios d) $(La/Sr)_N$ vs. Eu/Eu* ratios: the coexistence of high La/Yb ratios, low La/Sr ratios, and low Eu anomalies corroborate less plagioclase fractionation for the younger lavas; normalization values for La=0.348, Yb=0.249 and Sr=14, according to Leedy chondrite (Masuda *et al.*, 1973; Kay *et al.*, 1991).

that show reverse zoning. Therefore, for temperature estimates, averages of orthopyroxene and clinopyroxene compositions for each sample were calculated, considering rim and core compositions separately. The selected two-pyroxene geothermometers are not particularly pressure dependent, but where needed, (according to an average value obtained through geobarometry) a pressure value of 5kb was used for temperature calculations. Nevertheless, when applying geothermometers within a P range between 4 and 6kb, less than three degrees of temperature difference was obtained for each kb increment.

The range of calculated temperatures for each sample is consistent with the different geothermometers used. Overall, temperatures range between 970 to 850°C for both volcanic episodes of Cerro del las Tórtolas Formation (Table 6), with some particular exceptions. The main difference is seen for temperature calculations of samples from Zancarrón Cordillera (ZN162) which shows the highest temperatures, with values that range from 1140 to 920°C. For most of the methods used, samples from Zancarrón show the highest estimated temperatures.

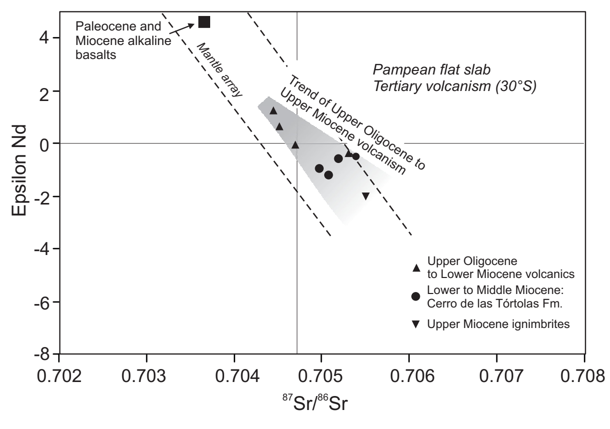

FIGURE 11. Isotopic evolution from Upper Oligocene to Upper Miocene magmas shows an increase in $^{87}Sr/^{86}Sr$ and decrease of εNd due to a higher degree of crustal-derived contributions for the younger magmas. Data from Kay *et al.* (1987, 1988, 1991, 1999) and Litvak *et al.* (2007).

In general, the Putirka (2008) and Fonarev and Graphchikov (1991) geothermometers produced consistently similar results and yielded temperatures between 960 to 900°C for samples from Brea Cordillera, Cerro Tórtolas and Despoblados, and higher values, between 1160 and 1000°C for those from Zancarrón. The Brey and Kholer (1990) and Lindlsey and Frost (1992) geothermometers –the latter calculated using the QUILF program– also produced consistent results, with values from 960 to 830°C for most of the areas, including Zancarrón samples that range from 970 to 930°C (Table 6). These two last geothermometers give consistent ranges for all samples including those from Zancarrón.

No major differences are seen between estimated temperatures of core and rim, thus reflecting the substantial homogeneous composition of the crystals. However, sample SP79, which has both orthopyroxene and plagioclase crystals with reverse zoning, has an anomalously lower core temperature value of 752°C, calculated with the Fonarev and Graphchikov (1991) method. This might be related to the higher Fe content of the orthopyroxene with respect to the composition of pyroxenes in the other samples. This effect is not seen when applying the other thermometers. The same happens in sample DI040, with a core temperature value of 765°C estimated with the Lindlsey and Frost (1992) method, which, in this case, could be related to an anomalously low Ca content of the orthopyroxene in the sample. Overall, estimated equilibrium temperatures yielded expected values for pyroxene crystallization in volcanic suites.

In order to check the two-pyroxene geothermometers results, the amphibole-plagioclase geothermometer calibrated by Holland and Blundy (1994) and amphibole geothermometer by Ridolfi *et al.* (2010) were applied to the samples from Cerro Tórtolas and Despoblados (from the older volcanic episode) and Cerro Tórtolas (from the younger one). Amphibole-plagioclase temperatures following Holland and Blundy (1994) were calculated for 5 and 6kb, according to previously estimated pressure values using average compositions of the amphibole and plagioclase. Most of the estimated temperatures are within the range of two-pyroxene geothermometers (samples DI040 and MQ28), with an overall range of 895 to 980°C (Table 7). No significant variation is seen either from values from the core or from the rim within each sample. However, one of the samples from the Lower Miocene volcanic episode of Cerro de las Tórtolas shows higher estimated temperatures with respect to the previous range (SP29: 1344 to 1030°C). This variation is strongly controlled by the anortite composition of the assemblage: higher T values from the Despoblados area (SP29) correspond to higher XAn (0.748-0.833), whereas T values from the Cerro Tórtolas (DI040 and MQ28) show XAn contents of 0.476-0.520. The estimated temperatures following Ridolfi *et al.* (2010) also yielded values consistent with amphibole-plagioclase and two pyroxenes geothermometers. In particular, the results show a temperature range between 976 and 943°C ± 22°C.

DISCUSSION

Origin of arc-related magmas

An Andean type arc was developed in the Upper Oligocene (~ 5Ma), at the Andean margin of present Pampean flat slab region, resulting in an almost continuous volcanic activity until the Upper Miocene (Kay *et al.*, 1987; 1991, 1999; Ramos *et al.*, 1989; Otamendi *et al.*, 1994; Bissig *et al.*, 2003; Litvak *et al.*, 2007).

In this context, the early to middle Miocene Cerro de las Tórtolas Formation, a calc-alkaline mesosilicic arc sequence, represents the peak of this magmatism, originated by the activity of the Cerro the Las Tórtolas and Vacas Heladas eruptive centers. Primary arc-related melts were generated in the asthenospheric wedge and later equilibrated at depth with different residual mineral assemblages, as originally proposed by Kay *et al.* (1987, 1988, 1991). Geochemically, two groups of volcanic rocks are recognized, mainly by the increase in the Sm/Yb ratio from the Lower to the Middle Miocene, which reflect an increase in pressure condition where magmas were firstly equilibrated at the base of the crust, as the mafic, residual mineralogy left at crustal depth changes from pyroxene to amphible to garnet (Kay *et al.*, 1999). Isotopic data also follow this trend; the upper section is more enriched in radiogenic Sr than the lower, as a result of the higher degree of crust-derived contributions.

The chemical evolution of this Miocene volcanism in the Southern Central Andes indicates changes in the residual mineral assemblages and variations in isotopic signatures consistent with a gradual increase of crustal thickness (Ramos *et al.*, 1989; Kay *et al.*, 1991, 1999; Bissig

TABLE 6. Geothermometry for Miocene lavas using clinopyroxene and orthopyroxene empirical methods

Sample		Fonarev and Graphchikov (1991) [1,2] T (°C)	Brey and Köhler (1990) T (°C)	Lindsley and Frost (1992) [1] T (°C)	Putirka (2008) T (°C)
SP79	Rim	907	830	829 ± 59	928
	Core	750	841	829 ± 19	956
SP29	Rim	968	928	958 ± 31	952
	Core	991	962	982 ± 25	965
DI040	Rim	897	867	835 ± 47	913
	Core	912	910	763 ± 80	914
ZN162	Rim	1056	970	917 ± 73	1006
	Core	1137	947	923 ± 74	1013
MQ28	Rim	938	892	900 ± 30	935
	Core	927	900	836 ± 31	944

[1] Calculated for a pressure of 5 Kb; [2] error is ± 50°C.

et al., 2003; Litvak *et al*., 2007). The increase of crustal thickness is a direct consequence of the gradual shallowing of the subduction angle and the increase of the compressive regime, due to the subduction of the Juan Fernandez Ridge, which arrived at the northern extreme of the flat slab segment 18Ma ago according to Yañez *et al*. (2001).

It should be noted that crustal contributions in the Valle del Cura volcanic rocks could be related to both processes of crustal thickening and peaks of forearc subduction erosion. The extremely steep REE pattern of lavas and ignimbrites of Middle Miocene age (12Ma) could reflect an episode of accelerated forearc subduction erosion as the Chile Ridge arrived, coincident with periods of arc migration and maximum compressional regimes occurred in Middle Miocene (Kay and Mpodozis, 2002; Kay *et al*., 2005; Litvak *et al*., 2007).

Lower Miocene melts (represented by the Lower Miocene volcanic episode rocks of Cerro de las Tórtolas Formation) were generated in the asthenospheric wedge and equilibrated at the base of the crust with residual mineral assemblages that reflect a crust of relatively normal thickness (~ 30 to 35km; Fig. 12A). In contrast, Middle Miocene melts –resulting in the younger volcanic episode rocks– were equilibrated at higher depths, related to a thicker crust of approximately 50km (Fig. 12B). These younger melts were also volumetrically restricted with respect to the older melts and only registred as part of the Cerro the las Tórtolas and Vacas Heladas eruptive centers, because the volume of the asthenospheric wedge was reduced below the main arc due to shallowing of the subduction angle (Fig. 12C) (Kay and Abruzzi, 1996).

Evolution of melts through the crust

Once the Miocene magmas were equilibrated at the base of the crust, the melts evolved in a compressive tectonic regime across the crust towards intermediate magma chambers, where they continued differentiating through MASH (melting, assimilation, storage, and homogenization) processes (Hildreth and Moorbath, 1988; Kay *et al*., 1987) and where phenocrysts assemblages had crystallized. Given the difference in depth of magma equilibration site at the base of the crust seen between the Lower and Middle Miocene magmas, the main question is whether this fact has influenced the evolution of each melt through the crust and, hence, the resulting volcanic products.

The main petrographic difference between the Lower and Middle Miocene volcanics is that older lavas have clino- and orthopyroxene as main mafic phases, with subordinate amphibole, and plagioclase phenocrysts. Conversely, the younger lavas also have plagioclase as phenocrysts but amphibole is the predominant mafic mineral with minor clino- and orthopyroxene. In addition, the younger rocks have tridimite and higher fresh glass content in the groundmass.

Mineral chemistry showed that the phenocryst compositions of Lower and Middle Miocene lavas are substantially homogeneous within each analyzed mineral phase, not only between the lavas of both volcanic episodes, but also when analyzing geographical distribution of the lavas and their probable provenance from the recognized eruptive centers. Thus, samples from the Cerro de las Tórtolas volcano, Despoblados, Zancarrón Cordillera and Brea Cordillera show similar mineral chemistry composition in their phenocryst assemblage.

Plagioclase phenocrysts show compositional zoning, but without a clear trend. Most of the samples have oscillatory or normal zoning, while only one crystal from

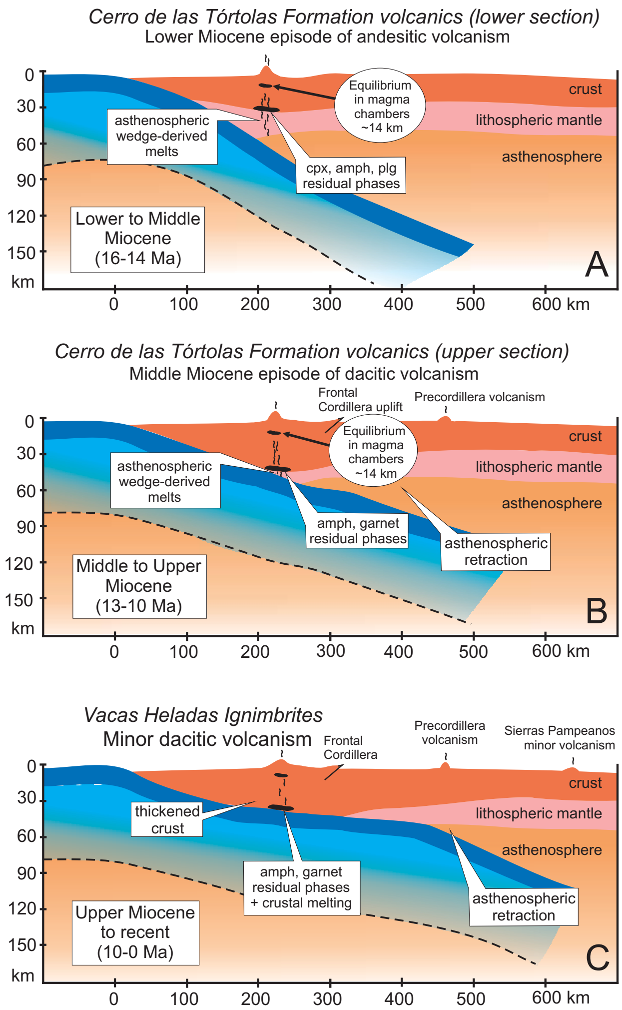

FIGURE 12. Geodynamical evolution of the Miocene magmatic history over the Pampean flat-slab segment, in a 29°-30° transect.

Zancarrón Cordillera shows a significative reverse one. Orthopyroxenes show normal zoning and only two of them, from La Brea and Zancarrón Cordilleras evidence reverse zoning, although compositional variations are not as notorious as that of plagioclase. Clinopyroxene composition is very homogenous in all the analyzed samples with a moderate dispersion of data. The same is observed for amphibole phenocrysts. Compositional variation seen in plagioclase could be related in part to self organization during crystal growth and/or to fluctuating external conditions, such as recycling of plagioclase through zones of cooler, more evolved melt, and hotter, more primitive melt in a convecting magma chamber or by influx of fresh magma in a more evolved resident magma (Gill *et al*., 2010). The relatively homogenous composition seen in pyroxene could evidence that they crystallized in a compositionally homogenous magmatic chamber. However, the external processes that might affected plagioclase crystallization, can also explain the reverse zoning seen in some of the orthopyroxenes.

In particular, the opaque ore rims around the amphiboles can be interpreted as decompression during magma ascent, because of the low survival rate of amphibole at low pressure (*e.g*. Shelley, 1993). This drop in pressure due to adiabatic ascent could also explain the groundmass corrosion seen in these amphibole phenocrysts (Gill *et al*., 2010). Nevertheless, changes in magma composition during amphibole crystallization, as mentioned for the plagioclase, could also explain the corrosion seen in amphibole phenocrysts.

Other textures, such as sieve textures in plagioclase and amphibole phenocrysts and the presence of two colored glasses in the same rock, which indicate mingling between distinct melts, also show that equilibrium was not kept during the entire formation of the rocks. Overall, these features indicate that phenocrysts were equilibrated in intermediate magmatic chambers affected by external processes. These desquilibrium processes have probably occurred in a local scale and related to local changes within the different magma chambers along the volcanic front, as they have partially affected the chemical composition of some of the phenocrysts, which in these particular cases is also reflected in the results of geothermobarometric estimates.

Amphibole geothermometer of Ridolfi *et al*. (2010) showed an overall temperature range of 970 to 943°C, which is within the range of two-pyroxene results (990 to 850°C). Most of the temperatures for the amphibole-plagioclase thermometers of Holland and Blundy (1994) are within Ridolfi´s range, but in some cases, higher values were obtained (overall, 1344 to 894°C) since they are strongly dependent on the An composition of the plagioclase phenocrysts.

Results of equilibrium pressure analyses show major variations according to the different methods. Classical Al-in hornblende thermometers originally applied in plutonic suites (Hollister *et al*., 1987, Schimdt, 1992) show higher values not particularly consistent with amphibole crystallization in a volcanic setting. One reason for these erroneous values could be related to the lack of the equilibrium assemblage needed for this method. Nevertheless, it should be noted that Tibaldi *et al*. (2011) on their study of metasedimentary migmatites, mentioned that the absence of these assemblages, when applying the thermometer, seemed to have little influence on the results. The Johnson and Rutherford (1989) geobarometer gave lower P values (~5kb), however, the lack of equilibrium assemblage could still explain the higher values. Finally, the Ridolfi *et al*. (2010) method gave the best results considering P and T crystallization equilibrium from amphibole (Helz, 1982), particularly for a volcanic suite. Although pyroxene might crystallize at higher T (~1100°C), textural features of both mafic minerals indicate that they were in equilibrium during crystallization.

Considering the density of the continental crust and the equilibrium pressure obtained from Ridolfi *et al*. (2010)

TABLE 7. Estimated temperatures for Miocene lavas from hornblende-plagioclase and hornblende thermometry, and pressure for Al-in-hornblende and hornblende geobarometry

Method			Holland and Blundy (1994)[1]				Ridolfi *et al.* (2010)[2]	Hollister *et al.* (1987)	Johnson and Rutherford (1989)	Schmidt (1992)	Ridolfi *et al.* (2010)
Sample		X An	T (°C) HB1 (5 Kb)	T (°C) HB2 (5 Kb)	T (°C) HB1 (6 Kb)	T (°C) HB2 (6 Kb)	T (°C)	P (kbar)	P (kbar)	P (kbar)	P (kbar)
DI040	Rim	0.527	970	929	954	930	943	5.84	4.49	5.94	2.76±30
DI040	Core	0.476	947	894	934	897	972	7.17	5.49	7.06	3.86±42
SP29	Rim	0.748	1183	1027	1166	1029	970	6.90	5.28	6.83	3.60±40
SP29	Core	0.833	1344	1095	1325	1097	968	6.78	5.20	6.73	3.51±39
MQ28	Rim	0.525	983	915	956	918	976	6.58	5.04	6.56	3.94±43
MQ28	Core	0.520	974	926	944	928	952	6.55	5.02	6.53	3.13±34

[1]HB1 is for Holland and Blundy (1994) geothermometer base on edenite-albite reaction, while HB2 is for edenite-anorthite reaction. [2] Error = ±22°C.

geobarometer (a value of 4kb), the equilibrium depth of the magma chambers can be estimated at 14km. As a result of the homogenous mineral composition between volcanic rocks from the Lower and Middle Miocene volcanic episodes, the same P and T conditions were obtained for the equilibrium of the mineral assemblages. So, despite the increase in depth of the magma equilibration at the base of the crust from the lower to upper section magmas –from Lower to Middle Miocene– equilibrium of phenocrysts was reached at the same depth and no deepening of the magma chambers is registered. Depth of magma chambers could have been controlled by the position of the brittle-ductile transition in the crust, which has also maintained at the same depth despite the increase in crustal thickness. Crustal pooling level of magma reservoirs were maintained at a relatively constant depth despite crustal thickening. This happened because shortening at a volcanic arc usually takes place at the lower crust, while the upper crust behaves as a rigid lid that is forelandward transported by the active structures of the fold and thrust belt. Thickening of the crust is produced at this part of the subductive configuration as lower crustal duplex systems, being the distance between surface and brittle-ductile transitions within the upper crust, where magma is stationary, relatively constant.

The final products of the studied Miocene volcanism were mainly influenced by processes seen in the magma chambers which were not directly affected by the depth of equilibration of the arc-related magmas at the base of the crust. Lower to Middle Miocene volcanics show petrographical differences that are mainly related to the magmatic differentiation processes that took place in the intermediate magma chambers within the crust: from basaltic-andesitic to andesitic lavas, in the Lower Miocene towards a more differentiated lava, andesitic to dacitic, in the Upper Miocene.

The higher content of amphibole in the younger lavas is related to these differentiation processes. As pointed out by Ridolfi *et al.* (2010) rocks with different bulk compositions (in this case, the lower and upper section lavas) brought to the same physico-chemical conditions produce similar amphibole compositions and different crystal percentages. Moreover, textural features that predominate in the Middle Miocene lavas, such as their dissolution textures and the high glass content, suggest possible lower residence times in the magma chambers for the magmas of this section.

CONCLUSIONS

Miocene volcanic arc magmatism in the Southern Central Andes over the Pampean flat slab is well represented by typical calc-alkaline andesitic to dacitic lava flows, which constitute high stratovolcanoes, together with pyroclastic deposits. Lava flows are included in the Cerro de las Tórtolas Formation that resulted from two volcanic episodes represented by a lower section of Lower Miocene age and an upper section of Middle Miocene age.

The main petrographic and chemical features and differences of the lava groups include: i) Lower Miocene lavas are volumetrically widespread all along the Valle del Cura, in contrast, the Upper Miocene lavas are restricted to the top levels of still preserved stratovolcanoes; ii) Petrographically, the older lavas are mostly basaltic-andesites to andesites, whereas younger lavas are dacites; iii) Chemically, the older lavas are also andesitic in composition in contrast with the younger lavas that are mostly dacites; iv) All of them show typical arc-like signatures according to their trace elements ratios and patterns; v) The younger melts, however, equilibrated at higher pressure conditions than the older melts, with garnet as a residual mineral phase, suggesting a deeper equilibration site at the base of the crust for the Middle Miocene magmas.

Despite particular variation in some specimens, mineral chemistry shows a relatively homogenous composition for the phenocryst composition of the lavas, which includes mostly oscillatory and normal zoned plagioclase, enstatitic orthopyroxene, augitic clinopyroxene and pargasitic amphibole, the latter more abundant as a mafic phase in the younger lavas. Equilibrium temperature conditions estimated through geothermometry show an overall temperature range between 970 and 850°C. Amphibole geobarometry for volcanic mineral assemblages show equilibrium pressure around 4kb. It should be noticed that consistent results were obtained for the different geothermometers and geobarometers applied, even though different mineral phases were used. Evolution of magmas and phenocrystal crystallization in intermediate magma chambers within the crust was reached at broadly the same pressure conditions. Consequently, no increase in the magma chambers' depth is indicated, despite the increase of crustal thickness between Lower to Middle Miocene times at these latitudes. In conclusion, we infer that the studied Miocene magmas were stationary at the same crustal pooling level.

ACKNOWLEDGMENTS

This research was supported by grant from the University of Buenos Aires (UBACYT 520). We thank the Cornell Center for Material Research (Cornell University, New York) for support in using the microprobe equipment and Dr. Suzanne Kay for her assistance in processing and discussing analytical results. US National Science Foundation Grant EAR0126000 provided funding. We thank Dr. Pablo Leal for the proof reading of the article and Dr. Andrés Folguera for discussion. We also thank two anonymous referees whose constructive reviews helped to improve the manuscript. This is paper number R-56 of the Instituto de Estudios Andinos Don Pablo Groeber (UBA-CONICET).

REFERENCES

Barckhausen, U., Ranero, C.R., Cande, S.C., Engels M., Weinrebe, W., 2008. Birth of an intraoceanic spreading center. Geology, 36(10), 767-770.

Bissig, T., Clark, A.H., Lee, J.K.W., Heather, K.B., 2001. The Cenozoic history of volcanism and hydrothermal alteration in the Central Andean flat-slab region: New 40Ar-39Ar constrains from the El Indio-Pascua Au-Ag-Cu belt, 29°20-30°30" S. International Geology Review, 43, 312-340.

Bissig, T., Clark, A.H., Lee, J.K.W, von Quadt, A., 2003. Petrogenetic and metallogenetic responses to Miocene slab flattenig: New constrains from the El Indio-Pascua Au-Ag-Cu Belt, Chile/Argentina. Mineralium Deposita, 38(7), 844-862.

Brey, G.P., Köhler, T., 1990. Geothermobarometry in four-phase lherzolites II. New thermobarometers, and practical assessment of existing thermobarometers. Journal of Petrology 31(6), 1353-1378.

Deer, W.A., Howie, R.A., Zussman, J., 1992. The rocks-forming minerals. Harlow, Logman Scientific & Technical, 2nd edition, 696pp.

Fonarev, V.I., Graphchikov, A.A., 1991. Two pyroxene thermometry: a critical evaluation. In: Perchuk, L.L. (ed.). Progress in metamorphic and magmatic petrology. Cambridge, Cambridge University Press, 65-92.

Helz, R.T., 1982. Phase relations and compositions of amphiboles produced in studies of the melting behaviour of rocks. Mineralogical Society of America Reviews in Mineralogy, 9B, 279-346.

Hildreth, W., Moorbath, S., 1988. Crustal contributions to arc magmatism in the Andes of Central Chile. Contribution to Mineralogy and Petrology, 98(4), 455-489.

Holland, T., Blundy, J., 1994. Non-ideal interactions in calcic amphibole and their bearing on amphibole–plagioclase thermometry. Contributions to Mineralogy and Petrology 116(4), 433-447.

Hollister, L.S., Grissom, G.C., Peters, E.K., Stowell, H.H., Sisson, V.B., 1987. Confirmation of the empirical correlation of aluminum in hornblende with pressure of solidification of calcalkaline plutons. American Mineralogy, 72(3-4), 231-239.

Jarosewich, E., Nelen, J.A., Norberg, J.A., 1980, Reference samples for electron microprobe analysis. Geostandards Newsletter, 4, 43-47.

Johnson, M., Rutherford, M., 1989. Experimental calibration of the Al-in-horblende geobarometer with application to Long Valley caldera (California) volcanics rocks. Geology, 17(10), 937-841.

Jones, J. P., Martínez, R., Rossello, E., 1996. La Faja volcánica terciaria del Valle del Cura (San Juan, Argentina): sus alcances y potencial para localizar World Class Deposits. In: Ramos, V.R., (ed.). Actas del XIII Congreso Geológico y III Congreso de Exploración de Hidrocarburos 3, Buenos Aires, 55-71.

Kay, M.S., Abbruzzi, J.M., 1996. Magmatic evidence for neogene lithospheric evolution of the Central Andes "flat slab" between 30°S and 32°S. Tectonophysics, 259, 15-28.

Kay, S.M., Gordillo, C.E., 1994. Pocho volcanic rocks and the melting of depleted continental lithosphere above a shallowly dipping subduction zone in the central Andes. Contributions to Mineralogy and Petrology, 117, 25-44.

Kay, S.M., Mpodozis, C., 2002. Magmatism as a probe to Neogene shallowing of the Nazca plate beneath the modern Chilean flat-slab. Journal of South American Earth Science, 15(1), 39-57.

Kay, S.M., Maksaev, V.A., Moscoso, R., Mpodozis, C., Nasi, C., 1987. Probing the evolving Andean lithosphere: Mid-Late Tertiary Magmatism in Chile (29°-30°30'S) over the modern zone of subhorizontal subduction. Journal of Geophysical Research, 92(B7), 6173-6189.

Kay, M.S., Maksaev, V.A., Moscoso, R., Mpodozis, C., Nasi, C., Gordillo, C.E., 1988. Tertiary Andean Magmatism in Chile and Argentina between 28°S and 33°S: Correlation of magmatic chemistry with changing Benioff zone. Journal South American Geology Earth Sciences, 1(1), 21-38.

Kay, S.M., Mpodozis, C., Ramos, V.R., Munizaga, F., 1991. Magma source variations for mid-late Tertiary magmatic rocks associated with shallowing zone and thickening crust in the central Andes (28° to 33°S). In: Harmon, R.S., Rapela, C.W. (eds.). Andean magmatism and its tectonic setting. Geological Society of America, 265 (Special Paper), 113-137.

Kay, S.M., Mpodozis, C., Coira, B., 1999. Neogene magmatism, tectonism and mineral deposits of the Central Andes (22º-23ºS latitude). In: Skinner, B.J. (ed.). Geology and Ore Deposits of the Central Andes. Society of Economic Geologists, 7 (Special Publication), 27-59.

Kay, S.M., Godoy, E., Kurtz, A., 2005. Episodic arc migration, crustal thickening, subduction erosion and magmatism in the South-Central Andes. Geological Society of American Bulletin, 117(1-2), 67-88.

Leake, B.E., Woolley, A.R., Arps, C.E.S., Birch, W.D., Gilbert, M.C., Grice, J.D., Hawthorne, F.C., Kato, A., Kisch, H.J., Krivovichev, V.G., Linthout, K., Laird, J., Mandarino, J.A., Maresch, W.V., Nickel, E.H., Rock, N.M.S., Schumacher, J.C., Smith, D.C., Stephenson, N.C.N., Ungaretti, L., Whittaker, E.J.W., Guo, Y., 1997. Nomenclature of amphiboles of the International Mineralogical Association, Commission on New Minerals and Mineral Names. American Mineralogist, 82(11-12), 1019-1037.

Limarino, C.O., Gutiérrez, P.R., Malizia, D., Barreda, V., Page, S., Ostera, H., Linares, E., 1999. Edad de las secuencias paleógenas y neógenas de las cordilleras de la Brea y Zancarrón, Valle del Cura, San Juan. Revista de la Asociación Geológica Argentina, 54(2), 177-181.

Lindsley, D.H., Frost, B.R., 1992. Equilibria among Fe-Ti oxides, pyroxenes, olivine and quartz: Part I. Theory. American Mineralogist 77(9-10), 987-1003.

Litvak, V.D., 2009. El volcanismo Oligoceno Superior–Mioceno Inferior del Grupo Doña Ana en la alta cordillera de San Juan. Revista de la Asociación Geológica Argentina, 64(2), 200-212.

Litvak, V.D., Poma, S., 2005. Estratigrafía y facies volcánicas y volcaniclásticas de la Formación Valle del Cura: magmatismo paleógeno en la Cordillera Frontal de San Juan. Revista de la Asociación Geológica Argentina, 60(2), 402-416.

Litvak, V.D., Poma, S., Limarino, C.O., 2004. Volcanismo piroclástico de edad miocena media en el Valle del Cura, provincia de San Juan: nuevos datos geológicos y geocronológicos. Revista de la Asociación Geológica Argentina, 59(3), 514-517.

Litvak, V.D., Poma, S., 2010. Geochemistry of mafic Paleocene volcanic rocks in Valle del Cura region: Implications for the petrogenesis of primary mantle-derived melts over the Pampean flat-slab. Journal of South American Earth Science, 29(3), 705-716.

Litvak, V.D., Chernicoff, C.J., Poma, S., 2005a. Localización de centros eruptivos mediante aeromagnetometría en el sector central del Valle del Cura, San Juan, Argentina: implicancias para la evolución de arco/retroarco Cenozoico. Revista Geológica de Chile, 32(1), 77-93.

Litvak, V.D., Kay, S.M., Mpodozis, C., 2005b. New K/Ar ages on tertiary volcanic rocks in the Valle del Cura, Pampean flat slab segment, Argentina. In: Llambías, E., de Barrio, R., González, P., Leal, P. (eds.). Actas del XVI Congreso Geológico Argentino 2, La Plata, 159-164.

Litvak, V.D., Page, S., 2002. Nueva evidencia cronológica en el Valle del Cura, provincia de San Juan. Revista de la Asociación Geológica Argentina, 57(4), 483-486.

Litvak, V.D., Poma, S., Kay, S.M., 2007. Paleogene and Neogene magmatism in the Valle del Cura region: a new perspective on the evolution of the Pampean flat slab, San Juan province, Argentina. Journal of South American Earth Science, 24(2-4), 117-137.

Maksaev, V., Moscoso, R., Mpodozis, C., Nasi, C., 1984. Las unidades volcánicas y plutónicas del Cenozoico superior entre la Alta Cordillera del Norte Chico (29°-31°S), Geología, alteración hidrotermal y mineralización. Revista Geológica de Chile, 21(1), 11-51.

Malizia, D., Limarino, C.O., Sosa-Gomez, J., Kokot, R., Nullo, F., Gutierrez, P., 1997a. Descripción de la Hoja Geológica Cordillera del Zancarrón, escala 1:100.000. Buenos Aires, Secretaría de Minería de la Nación, 280pp.

Martin, M.W., Clavero, J.R., Mpodozis, C.M., 1997a. Eocene to Late Miocene structural development of El Indio belt, 30°S, North-Central Chile. In: Universidad Católica del Norte (ed.). Actas del VIII Congreso Geológico Chileno 1, Antofagasta, 144-148.

Martin, M.W., Clavero, J.R., Mpodozis, C.M., 1997b. Eocene to Late Miocene magmatic development of El Indio belt, 30°S, North-Central Chile. In: Universidad Católica del Norte (ed.). Actas del VIII Congreso Geológico Chileno 1, Antofagasta, 149-153.

Masuda, A., Nakamura, N., Tanaka, T., 1973. Fine structures of mutually normalizad rare Herat patterns of chondrites. Geochimica et Cosmochimica Acta, 37, 239-248.

Miyashiro, A., 1974. Volcanic rock series in island arcs and continental margins. American Journal of Science, 274, 321-355.

Morimoto, N., 1989. Nomenclature of pyroxenes. Canadian Mineralogist, 43(1), 143-156.

Nasi, C.P., Moscoso, R.D., Maksaev, V.J., 1990. Hoja Guanta, Región de Coquimbo, Carta Geológica de Chile N° 67. Santiago de Chile, Servicio de Geología y Minería, 140pp.

Pardo Casas, F., Molnar, P., 1987. Relative motion of the Nazca (Farallón) and South America plates since Late Cretaceous time. Tectonics, 6(3), 233-248.

Peccerillo, A., Taylor, S.R., 1976. Geochemistry of Eocene calc-alkaline volcanic rocks from the Kastamonu area, northern Turkey. Contributions to Mineralogy and Petrology, 58, 63-81.

Putirka, K., 2008. Thermometers and barometers for volcanic systems. In: Putirka, K., Tepley III, F. (eds.). Minerals, Inclusions and Volcanic Processes. Reviews in Mineralogy and Geochemistry, Chantilly, Mineralogical Society of American, 69, 61-120.

Ramos, V.A., Kay, S.M., Page, R., Munizaga, F., 1989. La Ignimbrita Vacas Heladas y el cese del volcanismo en el Valle del Curá, província de San Juan. Revista de la Asociación Geológica Argentina, 44(1-2), 336-352.

Ramos, V.A., Cristallini, E.O., Pérez, D.J., 2002. The Pampean flat-slab of the Central Andes. Journal of South American Earth Sciences, 15(1), 59-78.

Ridolfi, F, Renzulli, A, Puerini, M., 2010. Stability and chemical equilibrium of amphibole in calc-alkaline magmas: an overview, new thermobarometric formulations and application to subduction-related volcanoes. Contributions to Mineralogy and Petrology, 160(1), 45-66.

Schmidt, M., 1992. Amphibole composition in tonalite as a function of pressure; An experimental calibration of the Al-in-hornblende barometer. Contributions to mineralogy and petrology, 110(2-3), 421-423.

Shelley, D. 1993. Igneous and metamorphic rocks under the microscope: classification, textures, microstructures and mineral preferred orientation. Springer, 445 pp., Chapman and Hall, London.

Tibaldi, A.M., Álvarez-Valero, A.M., Otamendi, J.E., Cristofollini, E.A., 2011. Formation of paired pelitic and gabbroic migmatites: An empirical investigation of the consistency of geothermometers, geobarometers and pseudosections. Lithos, 122(1-2), 57-75.

Winocur, D., 2005. Geología y estructura de la región de los Despoblados, Provincia de San Juan. Licenciatura Thesis. Buenos Aires, Universidad de Buenos Aires, 123pp.

Winocur, D.A., Litvak, V., Ramos, V.A., 2014. Magmatic and tectonic evolution of the Oligocene Valle del Cura basin, Main Andes of Argentina and Chile: Evidence for generalized extension. In: Sepúlveda, S., Giambiagi, L., Pinto, L., Moreiras, S., Tunik, M., Hoke, G., Farías, M. (eds.). Geodynamic Processes in the Andes of Central Chile and Argentina. Geological Society of London, 399 (Special Publications), http://dx.doi.org/10.1144/SP399.2

Yañez, G.A., Ranero, C.R., von Huene, R., Díaz, J., 2001. Magnetic anomaly interpretation across the southern central Andes (32°–34°): the role of the Juan Fernández Ridge in the late Tertiary evolution of the margin. Journal of Geophysical Research, 106(B4), 6325-6345.

Manuscript received August 2012;
revision accepted April 2014;
published Online May 2014.